COMPARATIVE EVALUATION OF ANTICANCER AND ANTIBACTERIAL ACTIVITIES OF ENDOPHYTIC FUNGUS-DERIVED ZNO NANOPARTICLES AND CHEMICALLY SYNTHESIZED ZNO NANOPARTICLES

Sameh Ezzat Hammad[1], *Hussein Hosny Elshikh [1], Mahmoud Nour Eldin EL-Rouby[2], Marwa Abdel-Aziz Mostafa[3].

[1]Department of Botany and Microbiology, Faculty of Science (Boys), Al-Azhar University, 11884 Nasr, Cairo, Egypt.

[2] Department of Cancer Biology, Egyptian National Cancer Institute, Cairo University,

Elkaser Alainy, Cairo, Egypt.

[3]Medical Microbiology, Regional Center of Mycology and Biotechnology, Al-Azhar University, Cairo, EGYPT;

***Corresponding author E-mail**: hussienhossny.221@azhar.edu.eg

ABSTRACT

Depending to the WHO, antibiotic resistance and limited anticancer and antimicrobial therapies continue to be serious worldwide health challenges. Current medicines' efficacy suffers by issues such as insufficient solubility, stability, and side effects. To create effective and dependable therapies against antibiotic resistance and robust illnesses, new techniques and strategies are required. Several metal nanoparticles synthesised via green synthesis or chemical synthesise, such as gold (Au), zine (ZnO), and others, have shown promising biological effects against malignancies and a wide spectrum of microbial illnesses caused by multi-drug resistant bacteria.

An eco-friendly biosynthetic technique was used to create zinc oxide nanoparticles (ZnO NPs), as well as their antibacterial and anticarcinogenic activities. Extracellular synthesis of nanoparticles made of zinc oxide ZnO nanoparticles was achieved in the current work using the cell filtrate of the endophytic fungus *Fusarium chlamydosporum* MW341592.1 isolated from healthy leaves of *Eucalyptus sideroxylon* plant. The nanoparticles were characterised by UV-VIS spectroscopy, X-ray diffraction (XRD), dynamic light scattering (DLS), transition electron microscopy (TEM), and energy-dispersive X-ray spectroscopy (EDX). The UV-Vis absorption spectra of the produced ZnO NPs showed bands in the UV area at (305) nm. Transmission electron microscopy TEM revealed average sizes of 19.3 nm, while shape revealed spherical like shape. The distinctive pattern of crystalline ZnO NPs was revealed by XRD diffract grams. Furthermore, Biological assay has shown that raising the nanoparticle concentration lowers the number of HCT-116 human colon cancer cells and CACO2 human intestinal cancer cells, as well as antibacterial pathogens *Escherichia coli and Pseudomonas aeruginosa.*

Keywords: zinc oxide nanoparticles, biosynthesis, endophytic fungus, antibacterial activity, anticancer activity

Introduction

During the previous decade, nanotechnology has emerged as a technology that has altered every field of applied science. The field of nanoparticles (NPs), which is associated with nanostructured materials with very small particle sizes varying from 1nm to 100 nm, is one of the approaches to nanotechnology. Because of their small size and high surface area to volume ratio, NPs have distinct characteristics than their bulk counterparts, resulting in

significant differences in features (**Mohd *et al.*, 2019**). Nanotechnology research has recently become a priority topic at the forefront of contemporary research in a variety of domains such as medicine, physics, chemistry, biology, and so on (**Zak *et al.*, 2011**).

Nanomedicine is the use of nanotechnology to treat, diagnose, monitor, and control illnesses. Despite recent medical improvements, several disorders, including AIDS (**Moyer *et al*., 2014),** tumor (**Mozaffari *et al.*, 2016),** bacterial infections (**Imani and Safaei 2019**), diabetes (**Wong *et al*., 2019),** chronic pain (**Sharifi *et al*., 2017),** and autoimmune disorders (**Mozaffari *et al* 2019)**, remain untreated. Because nanoparticles are the cornerstone of nanotechnology, their use in medicine has opened up new avenues for treatment (**Chen *et al*., 2010).**

Solvothermal, microemulsion, microwave aided, sonochemical, and chemical reduction in aqueous or non-aqueous solution are some of the physical and chemical methods used in nanoparticle production (**Kołodziejczak *et al.*, 2014, Ong *et al*., 2018**). Chemical and physical NPs synthesis methods have become popular in recent years due to the use of less energy during metal reduction and the formation of homogenous NPs with high accuracy **(Albanese *et al*., 2012)**. Thus, typical NPs synthesis methods are arduous, time consuming, dangerous, and rely on the use of toxic compounds that are unhealthy (cytotoxic, genotoxic, carcinogenic) and function as potent environmental pollutants **(Arshad *et al.*, 2017).**

Furthermore, due to their instability and toxicity, the biological uses of NPs derived through chemosynthesis have been limited **(Shah *et al*., 2015).** As a result, there is a difficult scientific necessity to identify alternate green sources to address these disadvantages. The hardest job in green synthesis of metal nanoparticles is to identify an appropriate and nontoxic natural product, as well as an eco-friendly solvent solution **(Ljaz *et al*., 2017).**

The three key processes in the manufacture of nanoparticles that should be considered from the standpoint of green chemistry are the choice of the solvent medium utilised for the synthesis, an ecologically benign reducing agent, and a nontoxic substance for nanoparticle stabilisation. The majority of synthetic methods documented to date rely significantly on organic solvents, which have a negative impact on the environment and are not safe for humans **(Parashar *et al*., 2009).**

Green synthesis employing plant extracts or microorganisms is a clean method since no hazardous chemicals are used in the production process; also, the synthesis process happens under moderate pressure and temperature conditions and at a lower cost **(Mukherjee *et al*., 2008).** Using many sorts of biological systems, eco-friendly and low cost methods might be developed. These are referred to as 'biological techniques of synthesis,' and they involve bacteria, fungi, yeasts, microalgae, macro algae, and plant extracts **(Saratale *et al*., 2018).**

Endophytes are fungal or bacterial members that live inside plant tissues for brief periods of time or throughout the plant's life cycle without negatively affecting the host plant **(Rana *et al*., 2020).** *E. robusta* possesses pharmacological efficacy, particularly in cancer and inflammation, as well as antioxidant and antibacterial properties (98). *Bacillus cereus* **(Sunkar & Nachiyar, 2012),** *Pseudomonas veronii* **(Baker and Satish 2015),** *Colletotricum sp*. **(Shankar *et al*., 2003),** P*encillium citrinum* **(Alappat *et al*., 2012),** *Aspergillus fumigatus* **(Bala and Arya 2013**), *Rhodococcus sp*. (**Ahmad *et al*.,2003**), and *Saccharomonospora sp*. **(Verma *et al*.,2013**) are among the endophytic microorganisms widely recognised for their capacity to synthesis NPs. *Eucalyptus* (Myrtaceae) plants have

been used in the manufacture of metal nanoparticles such as iron, silver, gold, and titanium **(Osmery *et al*., 2020).**

Bacteria have gained popularity due to their capacity to gather inorganic material both intracellularly and extracellularly. To counterbalance the stress caused by the presence of poisonous metal ions, certain bacterial strains convert harmful metal ions to nanoparticles as a defence mechanism **(Iravani 2014)**.

Like bacteria, fungi may store inorganic material both extracellularly and intracellularly (**Narayanan and Sakthive 2010**). Fungi may make bigger nanoparticles via external synthesis than through internal synthesis. Fungi's massive secretory components are engaged in nanoparticle reduction and capping. *Coriolus versicolor* (Ag-NP), *Penicillium fellutanum* (Ag-NP), *Fusarium oxysporum* (Ag-NP), Colletotrichum sp. (Au-NP), *Neurospora crassa* (Ag/Au-NP), *Fusarium oxysporum* (TiO_2), and Saccharomyces cerevisiae MTCC29 are examples of fungi used for nanoparticle manufacturing **(Salgado *et al*.,2019).**

Various chemical and physical methods are used to create ZnO NPs. Nonetheless, these methods are costly and harmful to the environment. As a result, the biosynthesis of ZnO NPs has lately advanced fast, with microorganisms that are cleaner, eco-friendly, non-toxic, and biocompatible as alternatives to chemical and physical methods **(Mohd *et al*., 2019).** Because of its biodegradability, low toxicity, and low cost, zinc oxide (ZnO) or zinc oxide nanoparticle (ZnO NP) has been employed in an increasing variety of commercial goods such as paint, coating, cosmetics, and biomedicine during the last two decades, notably in the anticancer or antibacterial domains **(Parihar *et al*., 2018).**

Metal oxide nanoparticles are used as antibacterial active materials. Because of its unique electrical arrangement and appropriate characteristics, ZnO is one of the new antimicrobial active materials **(Abebe *et al*., 2020).** Furthermore, because of their low cost, ease of production, and high electron mobility, ZnO nanostructures (nanorods, nanowires, and nanoflowers) **(Mishra *et al*., 2015)** are used in optoelectronic devices **(Haarindraprasad *et al*., 2015).** Zinc oxide nanoparticles are antimicrobial and inhibit microbe formation by entering the cell membrane. In Escherichia coli, it has been supported by an oxidative stress mechanism involving zinc oxide nanoparticles **(Zhang *et al*., 2007).**

Their low toxicity to human cells, low cost, size-dependent effective inhibition against a wide range of bacteria, capacity to prevent biofilm development, and even elimination of spores make them appropriate for use as anti-bacterial agents in fabrics **(Stankic *et al*., 2016)**. Interestingly, multiple investigations have found that ZnO-NPs are non-toxic to human cells **(Colon *et al*., 2006),** which has required their use as antibacterial agents, hostile to microorganisms, and have high biocompatibility with human cells **(Padmavathy and Vijayaraghavan 2008)**.

Many factors influence ZnO's antibacterial efficacy against bacteria, including the size of the NP, the concentration employed, and the kind of bacterium targeted (Gram-positive or Gram-negative) (**Yoo *et al*., 2021**). ZnO has been studied for its antibacterial efficacy against both Gram-positive and Gram-negative microorganisms, including *Escherichia coli* (*E. coli*), *Pseudomonas aeruginosa*, *Staphylococcus aureus* (*S. aureus*) and *Bacillus subtilis* **(Hussain *et al*., 2019).** One of the ZnO nanoparticle methods for bacterial inhibition is its capacity to dissolve the cell membrane (**Jacob *et al*., 2019**), which is caused by the production of reactive oxygen species (ROS) **(Shabaani *et al*., 2020).**

Zinc oxide nanoparticles are also used for selective cytotoxicity against cancer cells, displaying cytotoxicity via zinc-dependent protein activity imbalance and ROS production **(Shen *et al.*, 2013).** Zinc oxide nanoparticles show promise as anticancer therapeutics. ZnO nanoparticles are now being studied extensively for their anticancer effects.

The following are the characteristics of ZnO nanoparticles that have led to their increased use in anticancer treatment (**Bisht and Rayamajhi 2016) A**) ZnO nanoparticles have relatively high biocompatibility **(*Zhou et al.*, 2006) B)** Selectivity: When particularly in comparison to other nanoparticles, ZnO nanoparticles have an essential nature of showing selective cytotoxicity against cancerous cells in vitro **(Hanley *et al.*, 2008)** , C) Easy synthesis: Because of these different methods of synthesis, their size and size distribution can be easily controlled. **(Huang *et al.*, 2012), D)** increased cytotoxicity while exterior ZnO is biocompatible, greater intracellular ZnO dosages induces cytotoxicity through zinc-mediated protein activity disequilibrium and oxidative stress **(Shen *et al.*, 2013).**

ZnO nanoparticles have the unique ability to induce oxidative stress in cancer cells, which has been identified as one of the mechanisms of ZnO nanoparticle cytotoxicity towards cancer cells. This property is due to ZnO's semiconductor composition. When the cell's anti-oxidant capabilities is exceeded, ZnO promotes ROS generation, resulting in oxidative stress and, eventually, cell death **(Rasmussen *et al.*, 2010).** ZnO-NPs inhibit HT29, colon cancer cell growth in a dose-dependent way, change the membrane potentials, and limit colony formation **(Subramaniam *et al.*, 2019).** ZnO NPs shown antitumor efficacy against colon cancer HCT-116 cancer cells **(Majeed *et al.*, 2019).**

According to a WHO estimate, cancer represents one of the top causes of death and a major impediment to increasing life expectancy, accounting for ten million deaths in 2020. By 2040, the number of newly diagnosed cancer cases is estimated to rise to 29.5 million each year, with cancer-related fatalities rising to 16.4 million per year **(Ferlay *et al.*, 2018, Bray *et al.*, 2021).**

Traditional cancer therapies include chemotherapy and radiation, but all of these methods have substantial side effects due to their inability to differentiate malignant cells from healthy cells. Considering this, most patients are treated with a combination of surgical surgery, radiation, and chemotherapy. Because of the toxicity of anticancer drugs, poor selectivity, the potential of cancer recurrence, and the development of drug-resistant cancer cells, the use of these treatments is limited **(Chidambaram *et al.*, 2011).** Unfortunately, the existing cancer treatment and diagnostic procedures are inadequate and provide an insurmountable barrier, since many patients experience cancer recurrence and significant side effects. As a result, there is a growing demand for the discovery and identification of novel medications as anticancer treatment with minimal side effects **(Nabil *et al.*, 2020).**

Furthermore, a microbial infection causes almost 20% of all malignancies **(Smith *et al.*, 2014).** According to Safdar and Armstrong, bacteraemia is a major source of life-threatening complications in cancer patients, particularly those who take anti-cancer treatment. Because of inflammatory sores on mucosal surfaces and immune suppression caused by chemotherapy, cancer patients are more prone to invasive infection (**Safdar and Armstrong 2001**).

Many studies link Gram-negative bacteria to bloodstream infections in cancer patients **(Oliveira *et al.*, 2007).** *Pseudomonas aeruginosa* colonises the human gut frequently during hospitalisation, immunosuppression, antibiotic therapy, surgery, severe

trauma, and other situations that cancer patients may confront **(Markou and Apidianakis 2014).** *Pseudomonas aeruginosa* has long been recognised as one of the leading causes of severe sepsis and mortality in people with cancer having neutropenia **(Viscoli *et al*., 2005).**

Prognosis and is associated with the greatest mortality across different categories of people with bloodstream infections BSIs **(Kern *et al*., 2019).** Bacteria may trigger oncogenesis because they may create inflammation and generate cell-damaging toxins that promote cancer **(Collins *et al* 2011, Tjalsma *et al*., 2012).** Patel *et al*. identified colon cancer and shed light on the infectious proclivity of *E. coli* bacteremia to the development of colon adenocarcinoma **(Patel *et al*., 2017).** According to Hernández *et al*, some *E. coli* strains that produce the genotoxin colibactin have been linked to the development and progression of colon cancer **(Hernández *et al*., 2016). Buc *et al***. discovered cyclomodulin synthesis by *E. coli* from phylogenetic group B2 in biopsies from colon cancer patients, as well as pathways implicated in cancer formation **(Buc *et al*., 2013).**

MDR microorganisms continue to be the most difficult problem in public health care. Globally, the incidence of diseases caused by such resistant strains is growing. Pathogen acquired resistance is a significant concern for many antimicrobial medicines. Recent breakthroughs in nanotechnology provide new perspectives for developing unique formulations based on diverse types of nanoparticles (NPs) with varying sizes and shapes, as well as flexible antibacterial capabilities **(Baptista *et al*., 2018)**.

Aim of study

Green synthesis methods for the creation of metal nanoparticles are attracting a lot of attention. As a result, the goal of this work was to isolate endophytic fungi and investigate their extracellular capacity to synthesise, ZuO nanoparticles that outperform physical and chemical methods owing to ease of mass production and organism safety. This work was expanded to assess the antibacterial activity of the biosynthesetic and chemosynthetic ZnO NPs against selected cancers and associated strains of MDR pathogenic bacteria that cause infections that are fatal.

Materials and methods

Chemicals

All of the chemicals and reagents utilised in this investigation were of analytical grade and were not purified further. NanoTech for Photo-Electronics, City of 6 October, Al Giza, Egypt, supplied anhydrous zinc sulphate [$ZnSO_4$] and Chemosynthetic ZnO NPs. Crystal violet, Sigma sold dimethyl sulfoxide (DMSO) and trypan blue dye (St. Louis, Mo., USA).

Cell lines

VACSERA for Biological Products and Vaccines SAE, Giza, Egypt, provided the HCT-116 and CACO2 cell lines. All of the chemicals and microbiological medium used were of analytical quality and did not need to be purified further.

Microorganisms

Extended-spectrum Beta-lactamase According to the American Type Culture Collection, the *Escherichia coli* BAA-199 strain belongs to the SHV-3-ESBL class, which contains ESBL enzymes that confer resistance to extended-spectrum cephalosporins and monobactams.

Multiple drug resistance *Pseudomonas aeruginosa* BAA-2112 is a Gram-negative strain with resistance to up to 15 antibiotics, including penicillins, cephalosporins, carbapenems, quinolones, and aminoglycosides, according to the American Type Culture Collection. They were graciously provided by the National Research Center in Giza, Egypt.

Plant

Healthy *Eucalyptus sideroxylon* plant samples were obtained from desert research center to acquire endophytes separate, sterile polythene bags were utilized to transport healthy plant samples from their native habitat. According to Fisher and Petrini, the samples were transported into the laboratory and processed within 24 hours **(Fisher and Petrini 1987).**

Isolation of endophytic fungi

Healthy small cuttings some of *Eucalyptus sideroxylon* plant leaves were gathered. Entophytic fungi were isolated from plant parts using the technique described by **Hallman *et al*. (2006),** with the following modifications: To eliminate dust and dirt, healthy leaves were carefully cleaned under running tap water. Explants were washed well before being sliced into 0.5 cm x 0.5 - 1 cm slices without the midrib under aseptic conditions. Surface sterilisation of explants was achieved by immersing them in 70% ethanol for 30 seconds, followed by 3 minutes in a 13% commercial bleach solution (Clorox) (sodium hypochlorite solution), followed by three rinses with sterile distilled water. Explants were placed on sterile Petri dishes with sterile potato dextrose agar (PDA) treated with chloramphenicol (50 mg / L) to limit bacterial proliferation. All dishes were covered with par film and cultured at 28 °C for up to 7 days, following which emerging fungi were purified and transferred to fresh sterile PDA plates for another 7 days of incubation **(Suryanarayanan *et al*., 2003).**

Fungal biomass preparation

On a rotary shaker, all fungi were cultivated for 96 hours on malt extract broth at 28 ^{o} C. (120 rpm). The biomasses were collected by filtering them using Whatman filter paper No. 1 and then washing them in distilled water to remove any medium components. The biomass (25 gm wet weight) was placed in separate flasks with 100 ml of deionized water and incubated for 24 hours as previously described. The biomass was filtered, and the cell filtrate was collected and used to create nanoparticles.

Biosynthesis of nanoparticles

Separate manufacturing of Zn nanoparticles, 0.1 M, 1 mL of Zn SO4 was added to 10 mL of fungal filtrate, and the solutions were agitated for 24 hours in the dark at room temperature. Characterization of produced nanoparticles UV-visible spectrum of extracts depicts the green synthesis processes of ZnO NPs.

Identification of fungal isolates

Using an image analysis approach, the most potent fungal isolate was discovered at the Regional Center for Mycology and Biotechnology (RCMB) (Leica CTR 5000, 280 DFC). Endophytic fungus was transferred to malt extract medium and cultured for 7 days at 25°C with shaking (180 rpm). Centrifugation was used to gather mycelia, and DNA was recovered. PCR amplification of purified DNA was performed using primers ITS1 and ITS4. The sequences of fungal internal transcribed spacer ribosomal DNA (ITS-rDNA) were used to identify them. For ITS-rDNA amplification, a set of primers, ITS1 (5′-TCC GTAGGT GAA CCT GCG G-3′) and ITS4 (5′-TCC TCC GCT TGA TAT GC-3′) were

employed (White *et al*., 1990) (108), resulting in an ITS region amplicon of around 550 bp. The BLAST software, which is accessible on the National Center for Biotechnology Information website, was used to examine sequence data in the Gene Bank database (www.ncbi.nlm.nih.gov). To examine DNA similarities, the unknown sequence was compared to all of the sequences in the database (**Altschul *et al*., 1997**). Bio Edit software was used to assess alignment and molecular phylogeny. The PCR results for the isolate under examination were purified and sequenced at the Sigma Company of Scientific Service.

Characterization of Nanoparticles:

The optical property and morphology of NPs characterized using the following techniques for the purpose of general screening.

Optical Properties:

Ocean Optics USB2000+VIS-NIR Fiber optics spectrophotometer was used to acquire absorption spectra. The colour change of cell free filtrate when combined with Zn SO4 and HAuCl4 solutions was determined at wavelengths ranging from 300 to 800nm **(Vivek *et al*., 2012).** The fungal supernatant was used as a blank.

Size and Shape:

The transmission electron microscopy (HR-TEM) pictures were taken at the Nanotech Company for Photo-Electronic, Dreamland, Egypt, on October 6th. The HRTEM is a JOEL JEM-2100 at 200 kV with a Gatan digital camera Erlangshen ES500. **Domsch and colleagues (1993**). Sample photos were obtained in order to clearly demonstrate the particle makeup.

XRD patterns were created using an XPERT-PRO Powder Diffractometer system, with 2 theta (20^{O}-80^{O}), with Minimum step size 2Theta: 0.001, and a wavelength (Ka) of 1.54614^{O}.

Elemental Analysis**:** The EDX analysis is determined using an X-Max 80 detector unit equipped with a JEM-1230 transmission electron microscope for the detection of unique X-rays for elemental analysis (TEM).

Colloidal Properties: A Zeta-sizer (Model: Malvern Nano ZS Nano) DLS system equipped with a red (633 nm) laser and an Avalanche photodiode detector (APD) (quantum efficiency > 50 % at 633 nm) was used to determine the hydrodynamic diameter (HD) and Zeta-potential (Malvern Instruments Ltd., England). The samples were diluted 10 times with deionized water before being measured, and 250 ml of the suspension was transferred to a disposable low volume cuvette. After equilibration to a temperature of 25oC for 2 minutes, five measurements were taken using 12 runs of 10 seconds each **(Jans *et al*., 2009)**.

Cytotoxic effects of ZnO NPs

Cell line Propagation:

The cells were grown in Dulbecco's modified Eagle's medium (DMEM) supplemented with 10% heat-inactivated foetal bovine serum, 1% L-glutamine, HEPES buffer, and 50g/ml gentamycin. All cells were grown twice a week at 37oC in a humidified atmosphere with 5% CO2.

Cytotoxicity evaluation using viability assay:

For the cytotoxicity experiment, the cells were planted in a 96-well plate with 1 x 10^4 cells per well in 100ml of growth medium. After 24 hours, new medium containing varying amounts of the test sample was introduced. A multichannel pipette was used to apply repeated two-fold dilutions of the tested chemical component to confluent cell monolayers in 96-well flat-bottomed microtiter plates (Falcon, NJ, USA). The microtiter plates were incubated in a humidified incubator with 5% CO_2 for 24 hours at 37°C. Three wells were used for each concentration of the test material. Control cells were grown in the presence or absence of test sample and DMSO. The experiment was unaffected by the modest amount of DMSO (maximum 0.1%) included in the wells. After 24 hours of incubation at 37°C, the viable cell yield was determined using a colorimetric method. The absorbance at 490 nm was measured, and the percentage of living cells was calculated using the method below.

$$\%\ \text{of viability} = \frac{(\text{mean optical density of the tested sample after treatment})}{\text{The average optical density of untreated cells.}} \times 100.$$

Antimicrobial activity of biosynthesized ZnO NPs and Chemosynthetic ZnO NPs

Two Gram Negative MDR bacteria, *Escherichia coli* BAA-199 and *Pseudomonas aeruginosa* BAA-2112, were tested for antibacterial activity of the biosynthesized Au NPs and ZnO NPs against harmful bacteria. The MIC is the lowest antibacterial agent concentration that can suppress bacterial growth. According to Clinical and Laboratory Standards Institute (CLSI) recommendations, the MIC of biosynthesized ZnO NPs and Chemosynthetic ZnO NPs against bacteria was evaluated in a 96-well microtiter plate using 2,3,5-triphenyl tetrazolium chloride (**CLSI. 2017**) with some modifications from a previously described method by **Ashengroph *et al* 2020**. In brief, the bacterial culture was cultivated until it reached a Mc-Farland standard of 0.5. Following that, 10 ul of bacterial suspension was pipetted into wells containing 140 ul of nutritional broth with varying quantities of both chemosynthetic and biosynthetic ZnO NPs (0.12 to 31.25 g/mL). As a control, nutrient broth without ZnO NPs was provided. The microtiter plate was incubated at 37°C for 24 hours. After that, 10 L of 2,3,5-triphenyl tetrazolium chloride solution (20 mg/mL) was added to each well and incubated for 3 hours at 37°C. The MIC value was investigated in wells that did not produce a red colour. The measurements were taken in triplicate, and the average values SD were computed.

Results and discussion

Endophytic fungi are an exceptional source of natural bioactive compounds applicable in medicine and food industry moreover; they were used in synthesis of nanoparticles and nanomaterials. **(Sunkar and Nachiyar , 2013).** Our study was ongoing by isolation of fungal endophytes from leaves of *Eucalyptus sideroxylon* plant, the fungi grown out from plant tissues, were brought into pure culture on PDA.

For screening the potentiality of the isolated fungal endophytes for extracellular biosynthesis of ZnO NPs and Au NPs aqueous solution of of Zn SO_4, and $HAuCl_4$ (1mM) respectively were mixed with their filtrates. The color of the fungal filtrate was changed from light yellow to colorless after mixing with Zn SO_4 and from colorless to Violet color after mixing $HAuCl_4$ and this observation analysis was a preliminary identification of nanoparticles formation. **(Vivek *et al*., 2012)**

From 13 fungal isolates (from FI-01 to FI-013) only one fungal isolate (FI-03) was detected. This fungus was the most potent fungal strain for synthesis of Zn O NPs, then it

was identified at the Regional Center for Mycology and Biotechnology (RCMB) using image analysis system (Leica CTR 5000, 280 DFC).

18S rRNA, as shown in Figure 1 recognised the isolated fungus as *Fusarium chlamydosporum* based on macroscopic and microscopic traits, as well as molecular identification. As stated in Table 1, the DNA sequencing findings were submitted to GenBank with the accession number MW341592.1.

Table 1 shows the results of the molecular identification of *Fusarium chlamydosporum* endophytic fungus using 18S rRNA.

Accession Number	Identification	Accession Number Isolated by High Similarity	Highly Similarity Isolates	Identity %
MW341592.1	*Fusarium chlamydosporum* isolate	MH863977.1	*Fusarium verticillioides* culture CBS:126206 strain CBS Small subunit ribosomal RNA gene 126206, partial sequence	99.81

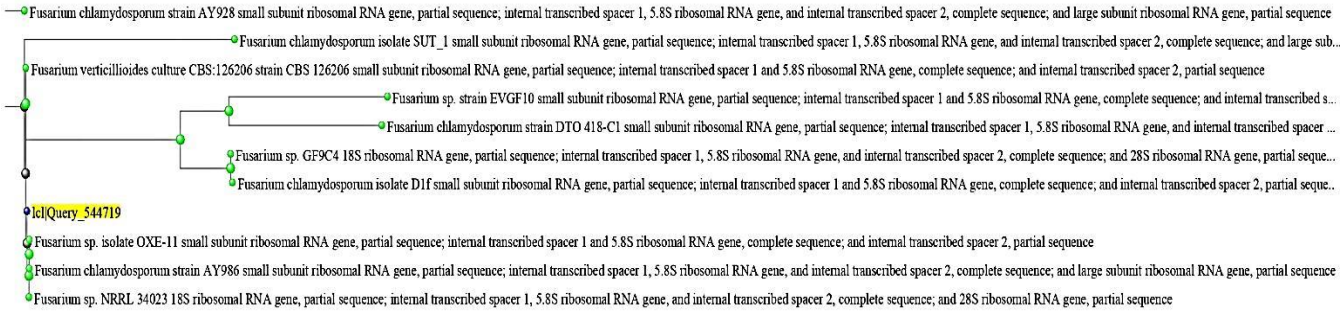

RNA sequencing (yellow highlighted).

2.2. Characterization of Biosynthesized ZnO NPs from *Fusarium chlamydosporum*

UV-Vis absorption spectra

The excitonic absorption peaks were between 300 and 400 nm, which are typical ZnO NPs peaks and hence establish their existence. The maximum absorption peak of ZnO NPs synthesized was 305 nm, demonstrating the synthesis of ZnO in a nano form (Figure 1); this finding is in good agreement with the previously reported values **(Aldalbahi *et al.*, 2020),** This is also consistent with recent findings showing that ZnO-NPs has a maximum absorbance wavelength in the region of 300-400 nm **(Kuruppu *et al.*, 2020** & **Wijesinghe *et al.*, 2021)**. A single, prominent absorption peak in the spectra confirms the existence of metallic gold nanoparticles (Figure 1). This finding is in agreement with **Iranmanesh *et al.* (2020).**

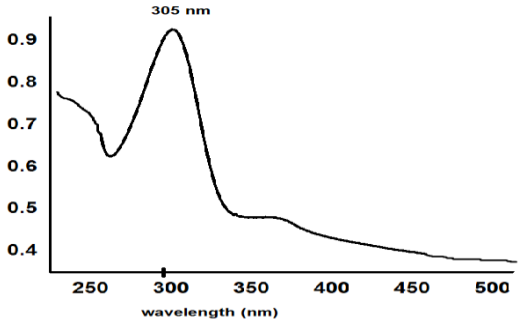

Figure 2 : UV-Visible spectral analysis of pure zinc oxide nanoparticles

Dynamic light scattering (DLS) analysis

A common approach for assessing particle size in colloidal solution is dynamic light scattering. It is used to calculate the thickness of the shell of a capping or stabilising chemical encapsulating the metallic nanoparticles as well as the actual size of the metallic core. According to the dynamic light scattering (DLS) and zeta-potential results, the hydrodynamic diameter (HD) of ZnO NPs is approximately 15.77 nm, and their corresponding polydispersity index (PdI) was approximately 1.00, which attributed to the highest tendency to be aggregated based on their hydrophilicity nature (Figure 3). According to **Clarance *et al*., 2020.**

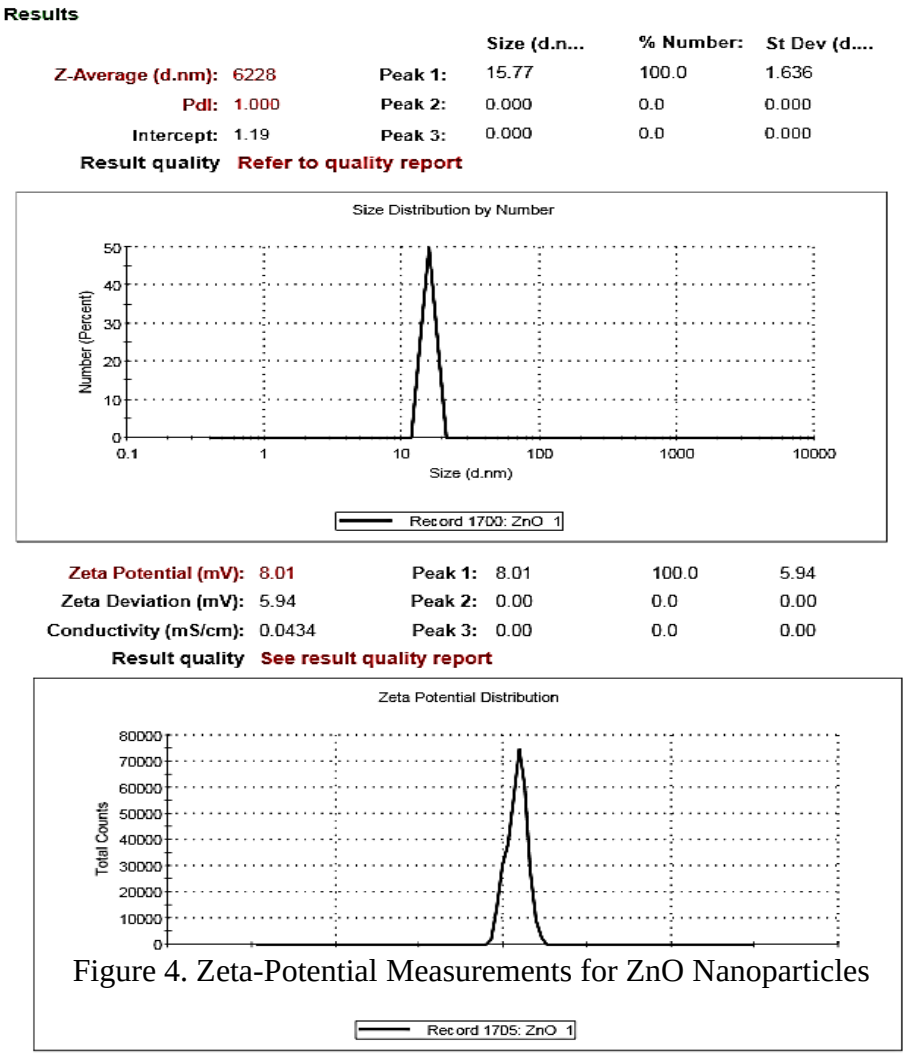

Figure 4. Zeta-Potential Measurements for ZnO Nanoparticles

Zeta potential (ZP) analysis

Zeta potential (ZP) analysis was carried out to detect surface charge and stability of Biosynthetic nanoparticles. The magnitude of zeta potential gives an insinuation of potential stability of colloid, the average ZP value of ZnO NPs was 8.01 mV as shown in Figure 4. In contrast, if the particles in a suspension have a large negative or positive zeta potential, there is no force to stop the particles from coming together and aggregating, and the zeta potential values are decreasing. If particles have small zeta potential values, they will repel one another and there will be no aggregation.

EDX Analysis of ZnO NPs

As illustrated in Figure 5, Zn and O the element mappings demonstrate that Zn and O are blended uniformly in the spheres. The spectrum displays peaks for Zn at 1.5, 8.5, and 9.6 MeV, as well as an O peak at 0.9 - 1.1 MeV, indicating that the NPs have a ZnO structure. Table 2 displays the composition line profiles.

Table 2. EDX elements of ZnO NPs

Element	Weight %
O (K)	35.39
Zn (M)	64.61
Totals	100.00

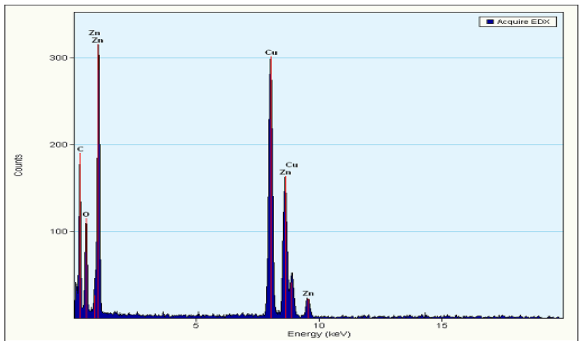

Figure 5. EDX mapping of biosynthetic A) ZnO.

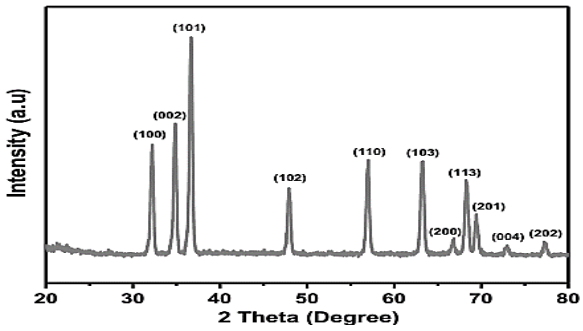

Figure 6 . XRD patterns for ZnO Nanoparticles

X-ray diffraction pattern for ZnO nanoparticles

The XRD pattern of as prepared ZnO NPs, show that the hexagonal structure is the predominant crystallographic structure according to (JCPDS No. 79-0205). The diffraction peaks with 2θ =31.76° (100), 34.58° (002), 36.67°(101), 47.89°(102), 57.01° (110), 63.29° (103), 66.67° (200), 68.25° (112), 69.35° (201), 73.27° (004) and 77.26° (202) correspond to the crystal plans of ZnO NPs were confirmed the hexagonal quartzite structure respectively. Here, no other impurity peaks are detected in the XRD patterns indicating that all products are rather purity of the nanoparticles formation as show in figure 6.

Morphological Properties (TEM and HR-TEM study Micrographs)

The result obtained from the TEM and HR-TEM study gave a clear indication regarding the shape, size and distribution of ZnO NPs. As shown in Fig. 7, 8 and Fig 8, the distance between two adjacent planes in ZnO was determined to be 2.772 Å (0.277 nm) and 2.267 Å (0.226 nm), corresponding to the (100) and (103) planes of wurtzite ZnO, respectively. The morphology and dimeter of the biologically synthesized ZnO NPs were determined by using Transmission electron microscopy (TEM). The images obviously show that the average dimeter of the particles was found to be in the order of 19.3 ± 5.0 nm.

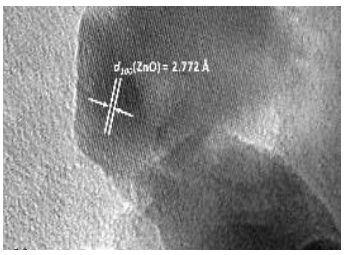

Figure 7.HR TEM micrographs of ZnO

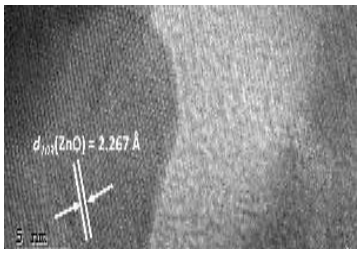

Figure 8. HR TEM micrographs of ZnO

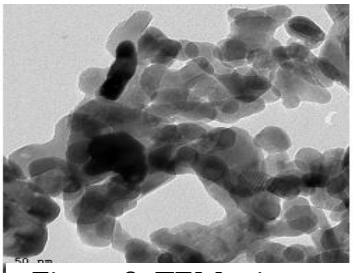

Figure 9. TEM micrographs of ZnO

Characterization of Chemosynthetic ZnO NPs :

Chemosynthetic ZnO was examined as provided from NanoTech for Photo-electronics which was white powder with spherical shape and average size 20 ± 5 nm.

Antibacterial Activity of biosynthesized nanoparticles

The emergence and rapid spread of antibiotic-resistant bacteria represent a serious global threat to human health, It is evident that the time and principal required for developing new antibiotics is great **(Meier, 2013)** NPs and bacteria *Escherichia coli* BAA-199 and *Pseudomonas aeruginosa* BAA-2112 are incubated in MHB. The concentration of inoculum of bacteria is around 1×105 CFU/ml. A range of NP concentration from 0.12 to 31.25 µg/ml was obtained by two-fold dilutions. After incubation for 24 h at 37 °C, the absorbance at 540 nm, which depends on the bacteria concentration, allows the evaluation of the bacteria growth.

Antimicrobial potential of the biosynthesized ZnO NPs nanoparticles was observed against microorganisms in contrast with $ZnSO_4.7H_2O$ as a control.

The minimum inhibitory concentration of biosynthesized ZnO NPs nanohybrids against the bacteria was studied using 2,3,5-triphenyl tetrazolium chloride in a 96-well microtiter plate, according to the Clinical and Laboratory Standards Institute (CLSI) guidelines, was examined against *P. aeruginosa* bacteria using different concentration (0.0, 0.12, 0.24, 0.49, 0.98, 1.95, 3.9, 7.81, 15.63 and 31.25 µg/ml) the mean of inhibition was (0.0, 14.3, 39.31, 51.43, 86.27, 100, 100, 100, 100,100) respectively as in table 3, While examined against *E.coli* was (0.0, 51.63, 79.35, 89.54, 100, 100, 100, 100, 100,100) respectively as in table 4. From Table 3 which indicates that the Minimum inhibitory concentration (MIC of biosynthetic ZnO NPs against *P. aeruginosa* was (1.95 µg/ml), whereas Table 4 showed that the Minimum inhibitory concentration (MIC of biosynthetic ZnO NPs against *E. coli* was (0.98 µg/ml).

Table 3. MICS of different biosynthetic Zn nanoparticles conc. against *P.aeruginosa*

Sample conc. (µg/ml)	Zn nanoparticles	
	Inhibitory percentage (%) ± SD	
	Mean of inhibitory %	SD
31.25	100	-
15.63	100	-
7.81	100	-
3.9	100	-
1.95	100	-
0.98	86.27	0.92
0.49	51.43	1.1
0.24	39.31	0.81
0.12	14.32	0.42
0	0	-
MIC (µg/ml)	**1.95**	

Table 4.MICS of different biosynthetic Zn nanoparticles conc. against *E. coli*

Sample conc. (µg/ml)	Zn nanoparticles	
	Inhibitory percentage (%) ± SD	
	Mean of inhibitory %	SD
31.25	100	-
15.63	100	-
7.81	100	-
3.9	100	-
1.95	100	-
0.98	100	-
0.49	89.54	0.63
0.24	79.35	1.3
0.12	51.63	0.58
0	0	-
MIC (µg/ml)	**0.98**	

Antibacterial Activity of chemosynthetic ZnO nanoparticles

The MIC of the chemo synthesized ZnO NPs against *P. aeruginosa* bacteria was examined using different concentration (0.0, 0.49, 0.98, 1.95, 3.9, 7.81, 15.63, 31.25, 62.5 and 125 µg/ml) the mean of inhibitory percentage was (0, 32.17, 41.25, 61.74, 86.32, 100, 100, 100, 100 and 100 %) respectively. While examination against E.coli was (0.0, 62.86, 82.17, 96.23, 100, 100, 100, 100, 100 and 100 %) respectively. Table 5 indicates that the Minimum inhibitory concentration (MIC of Chemosynthetic ZnO NPs against *P. aeruginosa* was (7.81 µg/ml), whereas Table 6 shows that the minimum inhibitory concentration (mic of chemosynthetic ZnO NPs against *E. coli* was (3.9 µg/ml).

Table 5.MICS of different conc. of chemosynthetic NPs against *P. aeruginosa*

Sample conc. (µg/ml)	Zn nanoparticles	
	Inhibitory percentage (%) ± SD	
	Mean of inhibitory %	SD
125	100	-
62.5	100	-
31.25	100	-
15.63	100	-
7.81	100	-
3.9	86.32	1.6
1.95	61.74	2.1
0.98	41.25	0.58
0.49	32.17	1.7
0	0	-
MIC (µg/ml)	**7.81**	

Table 6. MICS of different conc. of chemosynthetic NPs against *E.coli*

Sample conc. (µg/ml)	Zn nanoparticles	
	Inhibitory percentage (%) ± SD	
	Mean of inhibitory %	SD
125	100	-
62.5	100	-
31.25	100	-
15.63	100	-
7.81	100	-
3.9	100	-
1.95	96.23	1.3
0.98	82.17	0.58
0.49	62.86	1.2
0	0	-
MIC (µg/ml)	**3.9**	

Comparative between chemosynthetic and biosynthetic ZnO NPs against *P. aeruginosa and E.coli* bacteria

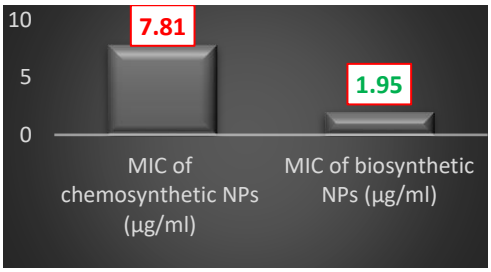

Figure 10.Comparative between chemosynthetic and biosynthetic ZnO NPs against P. aeruginosa

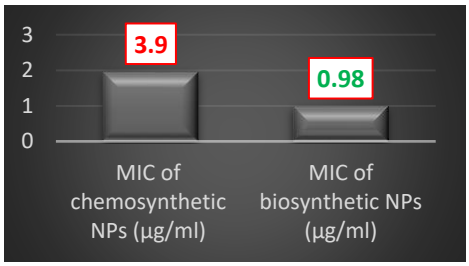

Figure11. Comparative between chemosynthetic and biosynthetic ZnO NPs against E.coli

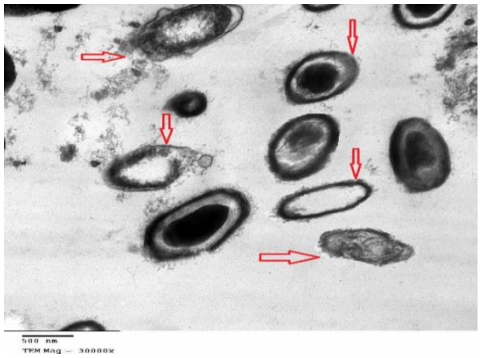

Figure 12. Effect of bioosynthetic ZnO against E.coli bacteria under TEM with magnification 30X

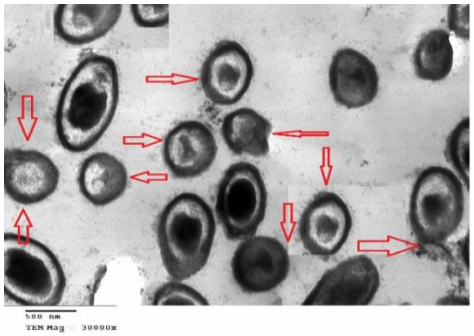

Figure 13. Effect of chemosynthetic ZnO against E.coli bacteria under TEM with magnification 30X

As in figures our results revealed that endophytic biosynthetic ZnO nanoparticles were better than chemosynthetic ZnO nanoparticles with the same shape and nearly sizable as antibacterial against multidrug resistance bacteria which make ZnO NPs a promising antibacterial agent. As mentioned by TEM in figure 12 and 13, the effect of chemosynthetic and biosynthetic ZnO NPs on *E. coli* is illustrated in the transmission electron microphotographs and the damage occurred by exposure the *E. coli* into ZnO NPs only and Au NPs individual.

Cells treated with the biosynthetic ZnO and visualized using conventional TEM showed increased morphological damage rather than chemosynthetic. Significantly, we observed a higher efficiency of these NPs to disrupt Gram-negative *E.coli.* These observations correlate well with the MIC studies where biosynthetic ZnO NPs shows superior antimicrobial activities compared to those of chemosynthetic ZnO NPs.

Anti-cancer activity ZnO NPs against HCT-116 and CACO2 cell

The cytotoxic effect of biosynthetic individual ZnO NPs against HCT-116 and CACO2 cell lines was investigated in this study, the 50% inhibitory concentration (IC50), the concentration required to cause toxic effects in 50% of intact cells.

Comparative between chemosynthetic and biosynthetic ZnO NPs against *colon cancer (HCT-116) cell line.*

Table 7.Evaluation cytotoxicity of NPs against colon cancer (HCT-116) cell line.

Conc. Of NPs (µg/ml)	Viability % in presence of	Viability % in presence of
0	100	100
0.05	100	100
0.1	100	100
0.2	100	100
0.39	100	100
0.78	98.42	98.64
1.56	85.16	91.47
3.125	63.74	78.2
6.25	41.55	53.12
12.5	28.94	37.68
25	16.43	24.95
50	7.59	11.82
100	4.61	6.79

Table 8. IC50 of chemosynthetic and biosynthetic ZnO NPs against colon cancer (HCT-116) cell line

Type of nanoparticles	Viability % in presence of biosynthetic ZnO NPs	Viability % in presence of chemosynthetic ZnO NPs
IC_{50} *µg/ml*	5.06	7.51

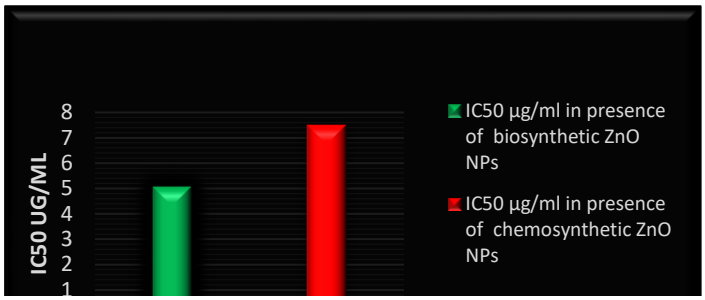

Figure 14. IC50 of chemosynthetic and biosynthetic ZnO NPs against colon cancer (HCT-116) cell line

Type	100 µg /ml	10 µg /ml	1 µg /ml
biosynthetic ZnO NPs		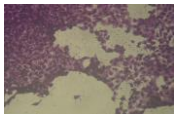	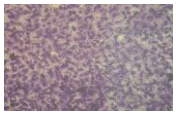
chemosynthetic ZnO NPs			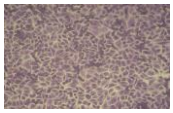
Control	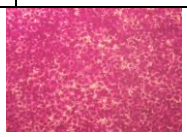		

Figure 15. Different Types of Nanoparticles Effects Against colon cancer (HCT-116) cell

From table 7.The toxicity of biosynthetic ZnO on HCT-116 cells increases dose-dependently, when treated with 0.0, 0.05, 0.1, 0.2, 0.39, 0.78, 1.56, 3.125, 6.25, 12.5, 25, 50 and 100 µg/mL of ZnO where the percentage of cell viability is reduced 100,100, 100, 100, 100 %, 98.42 %, 85.16 %, 63.74 %, 41.55 %, 28.94 %, 16.43, 7.59% and finally 4.61% respectively.

While in presence of Chemosynthetic ZnO NPs was reduced 100,100, 100, 100, 100 %, 98.64 %, 91.47 %, 78.2 %, 53.12 %, 37.68 %, 24.95, 11.82% and finally 6.79% respectively.

When comparing between the effect of chemosynthetic and biosynthetic ZnO nanoparticles against colon cancer (HCT-116) cell line we found that biosynthetic ZnO NPs was more effective than chemosynthetic ZnO NPs with inhibitory concentration (IC_{50}) 5.6 µg/ml while chemosynthetic was 7.51 µg/ml as demonstrated in table 8 and figure 14.

Morphological alterations of chemosynthetic nanoparticles effects against colon cancer (HCT-116) cell line

The effects of chemosynthetic and biosynthetic ZnOnanoparticles on colon cancer (HCT-116) cell line at varying concentrations were studied. The two types of nanoparticles

being evaluated. The concentrations tested are categorized as A) 1 µg/ml, B) 10 µg/ml, and C) 100 µg/ml., which show dose dependent effect highly at 100 µg/ml and the lowest one at 1 µg/ml for each NPs. (Figure 15).

Comparative between chemosynthetic and biosynthetic ZnO NPs against intestinsl cancer (CACO2) cell line.

The toxicity of ZnO NPs against CACO2 cells increases dose-dependently, when treated with 0.0, 0.05, 0.1, 0.2, 0.39, 0.78, 1.56, 3.125, 6.25, 12.5, 25, 50 and 100 µg/mL of ZnO NPs where the percentage of cell viability is reduced by 100,100, 100, 100, 96.03 %, 87.24 %, 70.81 %, 54.12 %, 32.39 %, 21.47%, 10.81, 6.53 and finally 2.74 % respectively

Table 9.Evaluation of cytotoxicity of NPs against Intestinal cancer (CACO2) cell line.

Conc. of NPs (µg/ml)	Viability % in presence of	Viability % in presence of
0	100	100
0.05	100	100
0.1	100	100
0.2	100	100
0.39	96.03	99.73
0.78	87.24	95.34
1.56	70.81	89.52
3.125	54.12	71.49
6.25	32.39	48.70
12.5	21.47	33.89
25	10.81	18.94
50	6.53	8.71
100	2.74	3.85

Table 10.IC50 of chemosynthetic and biosynthetic ZnO NPs against Intestinal cancer (CACO2) cell line

Type of nanoparticles	Viability % in presence of biosynthetic ZnO NPs	Viability % in presence of chemosynthetic ZnO NPs
IC_{50} µg/ml	3.7	6.07

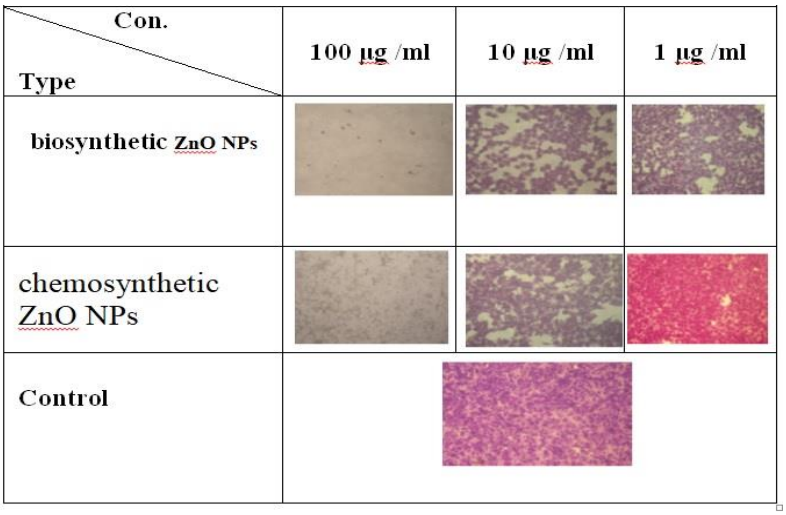

Figure 16.Different Types of Nanoparticles Effects Against intestinsl cancer (CACO2) cell line

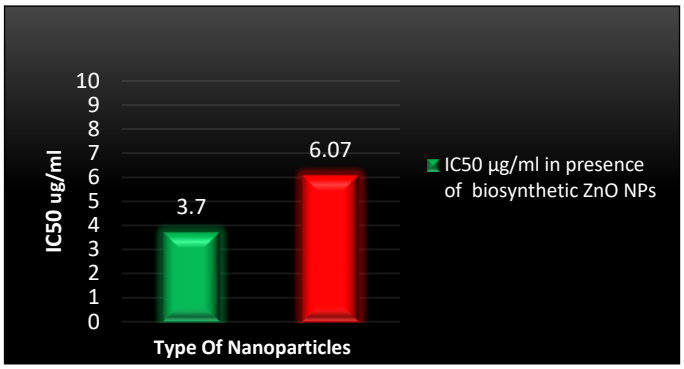

Figure 17.IC50 of chemosynthetic and biosynthetic ZnO NPs against Intestinal cancer (CACO2) cell line

While the percentage of cell viability is reduced by 100%,100%, 100%, 100%, 99.73%, 95.34%, 89.52%, 71.49%, 48.70%, 33.89%, 18.94%, 8.71 and finally 3.85% when treated with chemosynthetic ZnO NPs respectively. As in table 9.

When comparative between effect of chemosynthetic and biosynthetic ZnO nanoparticles against intestinal cancer CACO2 Cell line we found that biosynthetic ZnO NPs more effective than chemosynthetic ZnO NPs with inhibitory concentration (IC50) 3.7 µg/ml while chemosynthetic was 6.07 as demonstrated in table 10 and figure 16.

Morphological alterations of chemosynthetic Nanoparticles Effects against Intestinal Cancer CACO2 cell line

The effects of chemosynthetic and biosynthetic ZnO nanoparticles on Intestinal Cancer CACO2 cell line at varying concentrations. The two types of nanoparticles being evaluated. The concentrations tested are categorized as A) 1 µg/ml, B) 10 µg/ml, and C) 100 µg/ml., which show dose dependent effect highly at 100 µg/ml and the lowest one at 1 µg/ml for each NPs. Figure 17.

Ying *et al.*, 2022 said that green synthesis is more advantageous than traditional chemical synthesis because it is less expensive, reduces pollution, and enhances environmental and human health safety.

Nanoparticles exhibit completely new properties based on specific characteristics such as shape, size and distribution. These particles have many applications in the field of diagnostics, therapeutics and antimicrobials, catalysis and microelectronics **(Mishra *et al.*, 2014).**

Ibrahim *et al.*, 2016 in a previous studies on this genus endophytic fungus *Fusarium chlamydosporium* revealed that it is a wealthy source of biologically effective metabolites, including mycotoxins, cyclic depsipeptides, integracides, and naphthoquinones and pyrone derivatives.

A study published in the journal Materials Letters reported the synthesis of ZnO nanoparticles using *F. chlamydosporum* extract as a reducing and capping agent." **(Yousefi *et al.*, 2018).** Similarly, *F. chlamydosporum* has also been used for the synthesis of Au nanoparticles. **Bajpai *et al.*(2020).**

The current research shows a favourable relationship between an isolated fungi's zinc metal tolerance capacity and their potential for the creation of zinc oxide nanoparticles (ZnO-NPs). Thirteen fungal cultures were isolated from leaves of *Eucalyptus sideroxylon* plant and only one promising isolate, which capable to

synthesis of ZnO nanoparticles identified, based on macroscopic and microscopic characters, as well as molecular identification by 18S rRNA.

Jain *et al.* (2013) discovered that *A.aeneus* synthesised ZnO spherical nanoparticles coated with protein molecules that functioned as stabilising agents. They also demonstrated that the participation of fungal extracellular proteins in nanoparticle creation suggested that the process is nonenzymatic but requires amino acids found in protein chains. Several authors demonstrated the capacity of *A. fumigatus* **(Rajan *et al.*, 2016), *A. niger*** **(Kalpana *et al.*, 2018),** *F. oxysporum* **(Ahmad *et al.*, 2003),** *Fusarium chlamydosporum* **(Khalil *et al.*, 2019) and *P. citrinum*** **(Honary *et al.*, 2013)** to synthesis nanoparticles from metal salts.

Color change when *Fusarium chlamydosporium* is used for the biosynthesis of nanoparticles, it can lead to a distinct color change in the solution indicating the formation of the nanoparticles.

In our study, the first sign for the Endophytic fungus *F.chlamydosporum* aqueous extract biosynthesized of ZnO-NPs was a colour change from yellow to white precipitate. Which agreement with **Sharma *et al.* (2016)** said that the biosynthesis of zinc oxide (ZnO) nanoparticles from zinc ions can cause a change in color from colorless to pale yellow due to Surface Plasmon Resonance (SPR) effect.

Our study reported that the green synthesis of ZnO NPs by *F. chlamydosporum* are characterization using UV-Vis spectroscopy which observed a peak at around 305 nm similar to **Pandey *et al.* (2019)** which reported that the green synthesis and characterization of ZnO nanoparticles using UV-Vis spectroscopy. They observed that the absorbance spectra of the nanoparticles had a peak at around 375 nm, which was indicative of the presence of ZnO nanoparticles.

Our result revealed that the orientation and crystalline nature of zinc oxide nanoparticles. The peak position with 2θ values of 31.841˚, 34.507˚, 36.324˚, 47.592˚, 57.634˚, 62.895˚, 66.426˚, 67.983˚, and 69.091˚ are indexed as (100), (002), (101), (102), (110), (103), (002), (112), and (201) planes, which are in good agreement with similar study by **El-Rafie *et al.* (2015)** reported that the XRD analysis of the biosynthesized ZnO nanoparticles showed peaks at 2θ values of 31.77°, 34.39°, 36.16°, 47.61°, 56.57°, 62.97°, and 68.05°, which are attributed to the (100), (002), (101), (102), (110), (103), and (112) These results confirm the formation of crystalline ZnO nanoparticles with a hexagonal wurtzite structure.

Our study reveals DLS with mean average size of the NPs was about 97.8 nm. The size distribution profile of the ZnO NPs showed one significant peak with intensities of 100.0 %. The polydispersity index of the ZnO NPs was 0.367, which indicates that the synthesized particles had a little agglomeration and variation in size. This finding is completely compatible with **Ahmed *et al.* (2022)** and **Abdelbaky *et al*** **(2022)** who reported that PDI values of 0.3 and below are considered monodisperse, because of the hydrodynamical shell.

The study conducted by **Abdelbaky *et al.* (2022)** focused on the assessment of surface charges and stability of biosynthesized ZnO nanoparticles (ZnO NPs) through zeta potential (ZP) analysis. According to their findings, the

ZP value of the biosynthesized ZnO NPs was determined to be -19.3 mV. This negative ZP value indicates the potential stability of the nanoparticles.

In another study showed by **Ganesan *et al.* (2020),** the zeta potential and hydrodynamic particle size distribution of synthesized ZnO nanoparticles were investigated. The researchers observed a very high absolute zeta potential value of -88.6 mV, which indicated excellent stability of the nanoparticles. The zeta potential is a measure of the surface charge of particles, and a higher zeta potential leads to increased repulsion between particles, preventing agglomeration and contributing to higher stability.

Transmission electron microscopy (TEM) was used in this work to assess the shape and diameter of biologically synthesised ZnO NPs. The photos clearly reveal that the particles' average diameter was determined to be in the order of 19.3±5.0 nm and that they are reasonably uniform in diameter and spherical in shape). In another case, the crystalline structure of ZnO was studied using a selected area electron diffraction (SAED) pattern, which revealed five different rings indexed to the lattice planes 100, 002, 101, 110, and 103.

Ganesan *et al.* (2020) used transmission electron microscopy (TEM) to characterise the fabrication of zinc oxide (ZnO) nanoparticles. The TEM images indicated that the synthesised ZnO nanoparticles had a polydispersed distribution and an approximately spherical shape. The polydispersity index was discovered to be 1.48, indicating a considerable amount of size diversity among the nanoparticles. The particle size of the synthesised ZnO nanoparticles varied between 16 and 78 nm, which was commensurate with the average crystallite size derived from X-ray diffraction (XRD) research. The ZnO nanoparticles' selected area electron diffraction (SAED) pattern revealed circular peripheral layers corresponding to the polycrystalline planes (100), (002), (101), (102), (110), (103), (200), (112), and (201).

The current study mentioned biosynthesized ZnO NPs exhibited promising antimicrobial activity against both *Pseudomonas aeruginosa* and *Escherichia coli*. The minimum inhibitory concentration (MIC) values reflect the potency of the nanoparticles in inhibiting bacterial growth. For *P. aeruginosa*, the biosynthesized showed the MIC of ZnO NPs at 1.95 µg ml^{-1}, similarly, for *E. coli*, the biosynthesized ZnO NPs displayed the lowest MIC value of 0.98 µg ml^{-1}, µg ml^{-1}.

On the other hand, of chemosynthesized nanoparticles, the MIC values were slightly higher compared to their biosynthesized counterparts. The lowest MIC values for *P. aeruginosa* were observed for chemosynthesized ZnO NPs at 7.81 µg ml^{-1}, while for *E. coli*, the lowest MIC values were observed for chemosynthesized ZnO NPs at 1.95-µgml^{-1}.

Zubair and Akhtar (2020), in their study they revealed the antibacterial activity of the nanoparticles against three Gram-negative bacterial strains (*E. coli*, *P. aeruginosa*, and *Enterobacter cloacae*) and two Gram-positive bacterial strains (*S. mutans* and *S. aureus*). The results showed that the synthesized zinc oxide nanoparticles demonstrated promising antibacterial activity comparable to that of ciprofloxacin (positive control). The minimum inhibitory concentration (MIC) is the lowest concentration of an antimicrobial agent that inhibits the growth of a microorganism. The study did not report the MIC of the zinc oxide nanoparticles against the tested bacterial strains. However, the researchers used

three different concentrations (0.25, 0.50, and 0.75 µg/µL) of the selected zinc oxide samples and positive control to test the antibacterial activity.

Ganesan *et al.* 2020 reported that biosynthesized ZnO nanoparticles had high antibacterial efficacy against *Staphylococcus aureus* and *Escherichia coli.* Increasing the concentration of ZnO nanoparticles resulted in bigger inhibition zones, demonstrating a dose-dependent impact on microbial cell development. The minimum inhibitory concentration (MIC) and minimum bactericidal concentration (MBC) values revealed the efficiency of ZnO nanoparticles in suppressing the development of bacteria.

Mendes *et al* 2022 found that ZnO NPs reduced the development of *E. coli* and *P. aeruginosa* with IC100 values of 0.6 mM for both strains.As a result, *E. coli* and *P. aeruginosa* died at the lowest concentration of ZnO NPs, despite the fact that the current investigation found no significant variation in the IC values for Gram-negative bacteria. In a **2016** research**, Sharma** discovered that ZnO nanoparticles had significant antibacterial efficacy against *Pseudomonas aeruginosa* and *Staphylococcus aureus*, but not against *Klebsiella aerogenes* or *Pseudomonas desmolyticum* strains.

The antibacterial capabilities of nanoparticles are affected by their size, shape, and even manufacturing process. Typically, the smaller particle size allows ZnO nanoparticles to more easily enter bacteria, and hence their antibacterial action is stronger. (**Lallo *et al.,* 2019)**.

The work we have done has shown that nanoparticles (NPs) can reduce the viability of many malignant cell types. **Boroumand *et al.,* (2017)** demonstrated the effectiveness of NPs on MCF-7 breast cancer cells and MGC803 gastric cancer cells in comparison to other research. Furthermore, **Eid *et al.* (2020)** explored the effects of NPs on Caco-2 adenocarcinoma cells, while **Sisubalan *et al.,* (2018)** investigated their effects on MG-63 osteosarcoma cells. These findings show that nanoparticles have the potential to target and kill several types of cancer cells.

The current work investigated the toxicity of individual biosynthetic and chemosynthetic ZnO nanoparticles on the HCT-116 and CACO2 cell lines. The IC50 values, which represent the 50% inhibitory concentration, were computed for each type of NP.

The results revealed that the biosynthetic ZnO NPs exhibited lower IC50 values of 5.06 against the HCT-116 cell line and 3.7 against the CACO2 cell line. In contrast, the chemosynthetic ZnO NPs showed higher IC50 values of 7.5 for HCT-116 and 6.07 for CACO2. These findings suggest that biosynthetic ZnO NPs may possess stronger inhibitory effects on both cell lines compared to their chemosynthetic counterparts.

As reported by **Jasim and Saleh (2019)**, ZnO NPs produced cytotoxicity and morphological alterations in HCT-116 cells in a dose-dependent way. **Majeed *et al.,* (2019)** proved that bio-synthesized ZnO NPs generated considerable cytotoxicity against HCT-116 cells while being less harmful to Vero cells. Similarly, **El-Belely *et al.,* (2021)** discovered that ZnO NPs inhibited Caco-2 cell growth while inducing less toxicity in normal lung cells.

Bai *et al.* 2017 indicated that cell viability was significantly reduced after the application of 20 and 30 µg/mL ZnO NPs. **Mousa *et al.,* 2023** shown that green synthesis of ZnOnps is simple, inexpensive, non-toxic, and environmentally beneficial. Their

cytotoxicity on SKOV3 cells and the synthesised ZnO NPs resulted in a 50% inhibitory concentration (IC50) of 27.45 g/ml.

Al-dulaimi *et al.*, 2021 discovered that ZnO NPs have strong anticancer action, resulting in a loss of 82.5% in cell viability at low concentrations. Their efficacy is size-dependent, with a favourable relationship between lower cell viability and decreased toxicity.

A recent study by **Aljabali *et al,* 2022** shown that the cytotoxic impact of ZnO NPs was investigated against wild type and doxorubicin-resistant MCF-7 and MDA-MB-231 breast cancer cell lines. The results demonstrated the potential of ZnO NPs to suppress prefoliation of MCF-7 and MDA-MB-231 by inducing apoptosis without substantial differences in both wild type and resistance to doxorubicin.

Mousa *et al.*, 2023 shown that green synthesis of ZnO NPs is simple, inexpensive, non-toxic, and environmentally beneficial. Their cytotoxicity on SKOV3 cells and the synthesised ZnOnps resulted in a 50% inhibitory concentration (IC50) of 27.45 g/ml.

Conclusion

Finally, biosynthetic approach were used to successfully synthesise ZnO Nanoparticles by endophtic fungi. TEM, EDS, XRD, UV-vis, DLS, and zeta potential were used to confirm the green production of the aforementioned nanoparticles. According to the findings, *Fusarium chlamydosporum* extract could result in an environmentally friendly, large-scale, and continuous production of ZnO NPs (green synthesis). Furthermore, this ZnO NPs has antibacterial (MDR) and anticancer properties.

In conclusion, both biosynthetic and chemosynthetic nanoparticles have shown promising antibacterial effects against MDR bacteria. Biosynthetic nanoparticles generally exhibited higher potency with lower MIC values, while chemosynthetic nanoparticles had slightly higher MIC values.

Both biosynthetic and chemosynthetic nanoparticles have shown promising anticancer activity. However, results indicate that the biosynthetic nanoparticles generally showed lower IC50 values compared to their chemosynthetic counterparts, suggesting a higher potency and effectiveness in inhibiting the growth of both HCT-116 and CACO2 cancer cells.

REFERENCES

Abdelbaky, A. S., Abd El-Mageed, T. A., Babalghith, A. O., Selim, S., Mohamed, A. M. H. A. (2022). Green Synthesis and Characterization of ZnO Nanoparticles Using *Pelargonium odoratissimum* (L.) Aqueous Leaf Extract and Their Antioxidant, Antibacterial and Anti-inflammatory Activities. Antioxidants (Basel), 11(8), 1444. https://doi.org/10.3390/antiox11081444

Abebe, B., Zereffa, E. A., Tadesse, A., Murthy, H. C. A. (2020). A Review on Enhancing the Antibacterial Activity of ZnO: Mechanisms and Microscopic Investigation. Nanoscale Res Lett, 15(1), 190. https://doi.org/10.1186/s11671-020-03418-6

Ahmad, A., Mukherjee, P., Senapati, S., Mandal, D., Khan, M. I., Kumar, R., Sastry, M. (2003). Extracellular biosynthesis of silver nanoparticles using the fungus *Fusarium oxysporum*. Colloids and Surfaces B: Biointerfaces, 28(4), 313-318. ISSN 0927-7765

Ahmed, N., Elshemy, M. M., Asem, M., Abdel-Motaal, M., Gomaa, H. F., Zahran, F., Uto, K., Ebara, M. (2020). Zinc Oxide Nanoparticle Synergizes Sorafenib Anticancer Efficacy with Minimizing Its Cytotoxicity. Oxidative Medicine and Cellular Longevity, 2020, Article ID 1362104, 11 pages.

Alappat, C. F., Kannan, K., Vasanthi, N. (2012). Biosynthesis of Au nanoparticles using the endophytic fungi isolated from Bauhinia variegata L. Eng. Sci. Tech. Int. J., 2, 377–380.

Albanese, A., Tang, P. S., Chan, W. C. (2012). The effect of nanoparticle size, shape, and surface chemistry on biological systems. Annu. Rev. Biomed. Eng., 14, 1–16. https://doi.org/10.1146/annurev-bioeng-071811-150124

Aldalbahi, A., Alterary, S., Ali Abdullrahman Almoghim, R., Awad, M. A., Aldosari, N. S., Fahad Alghannam, S., Nasser Alabdan, A., Alharbi, S., Ali Mohammed Alateeq, B., Abdulrahman Al Mohsen, A., Alkathiri, M. A., Abdulrahman Alrashed, R. (2020). Greener Synthesis of Zinc Oxide Nanoparticles: Characterization and Multifaceted Applications. Molecules, 25(18), 4198

Al-dulaimi, M., Hammadi, M., Sabah, R. (2021). Anti-cancer activity of ZnO Nanoparticles on Hep-G2 and HCT-116 cells. 10.31838/ijpr/2020.12.03.055

Aljabali, A. A. A., Obeid, M. A., Bakshi, H. A., Alshaer, W., Ennab, R. M., Al-Trad, B., Al Khateeb, W., Al-Batayneh, K. M., Al-Kadash, A., Alsotari, S., Nsairat, H., Tambuwala, M. M. (2022). Synthesis, Characterization, and Assessment of Anti-Cancer Potential of ZnO Nanoparticles in an In Vitro Model of Breast Cancer. Molecules, 27(6), 1827.

Altschul, S. F., Madden, T. L., Schäffer, A. A., Zhang, J., Zhang, Z., Miller, W., & Lipman, D. J. (1997). Gapped BLAST and PSI-BLAST: A new generation of protein database search programs. Nucleic Acids Res., 25(17), 3389-3402. https://doi.org/10.1093/nar/25.17.3389

Arshad, A., Iqbal, J., Mansoor, Q., & Ahmed, I. (2017). Graphene/SiO_2 nanocomposites: The enhancement of photocatalytic and biomedical activity of SiO_2 nanoparticles by graphene. J. Appl. Phys., 121, 244901. https://doi.org/10.1063/1.4979968

Ashengroph, M., Khaledi, A., & Bolbanabad, E. M. (2020). Extracellular biosynthesis of cadmium sulphide quantum dot using cell-free extract of *Pseudomonas chlororaphis* CHR05 and its antibacterial activity. Process Biochem., 89, 63-70.

Bai, D.-P., Zhang, X.-F., Zhang, G.-L., Huang, Y.-F., & Gurunathan, S. (2017). Zinc oxide nanoparticles induce apoptosis and autophagy in human ovarian cancer cells. Int J Nanomedicine, 12, 6521.

Bajpai, V. K., Sharma, A., & Baek, K. H. (2020). Biosynthesis of gold nanoparticles using endophytic fungi isolated from Korean pine tree. Nano-Structures & Nano-Objects, 22, 100434. https://doi.org/10.1016/j.nanoso.2020.100434

Baker, S., & Satish, S. (2015). Biosynthesis of gold nanoparticles by Pseudomonas veronii AS41G inhabiting Annona squamosa L. Spectrochim. Acta A Mol. Biomol. Spectrosc., 150, 691-695.

Bala, M., & Arya, V. (2013). Biological synthesis of silver nanoparticles from aqueous extract of endophytic fungus *Aspergillus fumigatus* and its antibacterial action. Int. J. Nanomater. Biostruct., 3, 37-41.

Baptista, P. V., McCusker, M. P., Carvalho, A., Ferreira, D. A., Mohan, N. M., Martins, M., & Fernandes, A. R. (2018). Nano-Strategies to Fight Multidrug Resistant Bacteria—"A Battle of the Titans". Front. Microbiol., 9, 1441. https://doi.org/10.3389/fmicb.2018.01441.

Bisht G, Rayamajhi S. (2016) ZnO Nanoparticles: A Promising Anticancer Agent. Nanobiomedicine (Rij). Jan 1;3:9. doi: 10.5772/63437.

Boroumand Moghaddam, A., Moniri, M., Azizi, S., Abdul Rahim, R., Bin Ariff, A., Navaderi, M., & Mohamad, R. (2017). Eco-Friendly Formulated Zinc Oxide Nanoparticles: Induction of Cell Cycle Arrest and Apoptosis in the MCF-7 Cancer Cell Line. Genes, 8, 281. https://doi.org/10.3390/genes8100281

Bray, F., Laversanne, M., Weiderpass, E., & Soerjomataram, I. (2021). The ever-increasing importance of cancer as a leading cause of premature death worldwide. Cancer, 127, 2864-2866.

Buc, E., Dubois, D., Sauvanet, P., Raisch, J., Delmas, J., Darfeuille-Michaud, A., Pezet, D., & Bonnet, R. (2013). High prevalence of mucosa-associated *E. coli* producing cyclomodulin and genotoxin in colon cancer. PloS one, 8, e56964.

Chen, W. Y., Lin, J. Y., Chen, W. J., Luo, L., Wei-Guang Diau, E., & Chen, Y. C. (2010). Functional gold nanoclusters as antimicrobial agents for antibiotic-resistant bacteria. Nanomedicine (Lond), 5, 755-764.

Chidambaram, M., Manavalan, R., & Kathiresan, K. (2011). Nanotherapeutics to overcome conventional cancer chemotherapy limitations. J. Pharm. Sci. Pharmacol., 14(1), 67-77.

Clarance, P., Luvankar, B., Sales, J., Khusro, A., Agastian, P., Tack, J.-C., Al Khulaifi, M. M., AL-Shwaiman, H. A., Elgorban, A. M., Syed, A., & Kim, H.-J. (2020). Green synthesis and characterization of gold nanoparticles using endophytic fungi *Fusarium solani* and its in-vitro anticancer and biomedical applications. Saudi Journal of Biological Sciences, 27(2), 706-712.

Clinical and Laboratory Standards Institute (CLSI). (2017). Performance Standards for Antimicrobial Susceptibility Testing; Twenty-Seventh Informational Supplement; CLSI Document M100-S27. CLSI.

Collins, D., Hogan, A. M., & Winter, D. C. (2011). Microbial and viral pathogens in colorectal cancer. Lancet Oncol., 12, 504-512. https://doi.org/10.1016/S1470-2045(10)70186-8.

Colon, G., Ward, B. C., & Webster, T. J. (2006). Increased osteoblast and decreased *Staphylococcus epidermidis* functions on nanophase ZnO and TiO_2. Journal of Biomedical Materials Research Part A, 78(3), 595–604.

Domsch, K. H., Gams, W., & Anderson, T. H. (1993). Compendium of Soil Fungi. Academic Press.

Eid, A. M., Fouda, A., Niedbała, G., Hassan, S. E. D., Salem, S. S., Abdo, A. M., Hetta, H. F., & Shaheen, T. I. (2020). Endophytic *Streptomyces laurentii* mediated green synthesis of Ag-NPs with antibacterial and anticancer properties for developing functional textile fabric properties. Antibiotics, 9, 641. https://doi.org/10.3390/antibiotics9100641

El-Belely, E. F., Farag, M. M. S., Said, H. A., Amin, A. S., Azab, E., Gobouri, A. A., & Fouda, A. (2021). Green Synthesis of Zinc Oxide Nanoparticles (ZnO-NPs) Using Arthrospira platensis (Class: Cyanophyceae) and Evaluation of their Biomedical Activities. Nanomaterials, 11(1), 95. https://doi.org/10.3390/nano11010095

El-Rafie, H. M., El-Rafie, M. H., Zahran, M. K., & El-Samawaty, A. M. (2015). Green synthesis of Au–ZnO nanocomposites using fungal extract of Cunninghamella. Materials Science in Semiconductor Processing, 40, 540-545. https://doi.org/10.1016/j.mssp.2015.06.051

Elrefaeya, A. A., El-Gamala, A. D., Hamedb, S. M., El-Belelya, E. F. (2022). Algae-mediated biosynthesis of zinc oxide nanoparticles from Cystoseira crinite (Fucales; Sargassaceae) and its antimicrobial and antioxidant activities. Egypt. J. Chem., 65(4), 231-240.

Ferlay, J., Ervik, M., Lam, F., Colombet, M., Mery, L., Piñeros, M., Znaor, A., Soerjomataram, I., & Bray, F. (2018). Global cancer observatory: Cancer today. International Journal of Cancer, 144, 1941–1953.

Fisher, P. J., & Petrini, O. (1987). Location of fungal endophytes in tissues of *Suaeda fruticosa*: a preliminary study. Transactions of the British Mycological Society, 89, 246–249.

Ganesan, V., Hariram, M., Vivekanandhan, S., & Muthuramkumar, S. (2020). *Periconium* sp. (endophytic fungi) extract mediated sol-gel synthesis of ZnO nanoparticles for antimicrobial and antioxidant applications. Materials Science in Semiconductor Processing, 105, 104739. https://doi.org/10.1016/j.mssp.2019.104739

Haarindraprasad, R., Hashim, U., & Gopinath, S. C. B. (2015). Low temperature annealed zinc oxide nanostructured thin film-based transducers: characterization for sensing applications. PLoS One, 10(1), e0132755. https://doi.org/10.1371/journal.pone.0132755

Hallman, J., Berg, G., & Schulz, B. (2006). Isolation procedures for endophytic microorganisms. In B. Schulz, C. Boyle, & T. Sieber (Eds.), Microbial Root Endophytes (pp. 299-319). Springer-Verlag Berlin Heidelberg.

Hernández, M. A., Lagunes-Servin, H. E., Lopez-Briones, S. (2016). The role of *Escherichia coli* in the development and progression of cancer. ARC Journal of Cancer Science, 3(1), 1-11.

Honary, S., Barabadi, H., Gharaei-Fathabad, E., & Naghibi, F. (2013). Green synthesis of silver nanoparticles induced by the fungus *Penicillium citrinum*. Tropical Journal of Pharmaceutical Research, 12(1), 7-11.

Huang, K., Ma, H., Liu, J., Huo, S., Kumar, A., Wei, T., Liang, X. J. (2012). Size-dependent localization and penetration of ultrasmall gold nanoparticles in cancer cells, multicellular spheroids, and tumors in vivo. ACS Nano, 6(5), 4483–4493.

Hussain, A., Oves, M., Alajmi, M. F., Hussain, I., Amir, S., Ahmed, J., Rehman, M. T., El-Seedif, H. R., & Ali, I. (2019). Biogenesis of ZnO nanoparticles using *Pandanus odorifer* leaf extract: anticancer and antimicrobial activities. RSC Advances, 9(27), 15357–15369.

Ibrahim, S. R. M., Elkhayat, E. S., Mohamed, G. A. A., Fat'hi, S. M., & Ross, S. A. (2016). Fusarithioamide A, a new antimicrobial and cytotoxic benzamide derivative from the endophytic fungus Fusarium chlamydosporium. Biochemical and Biophysical Research Communications, 479(2), 211-216. https://doi.org/10.1016/j.bbrc.2016.09.041

Imani, M. M., & Safaei, M. (2019). Optimized Synthesis of Magnesium Oxide Nanoparticles as Bactericidal Agents. Journal of Nanotechnology, 2019, 6063832.

Iranmanesh, S., Shahidi Bonjar, G. H., & Baghizadeh, A. (2020). Study of the biosynthesis of gold nanoparticles by using several saprophytic fungi. SN Applied Sciences, 2, 185.

Iravani, S. (2014). Bacteria in nanoparticle synthesis: Current status and future prospects. International Scholarly Research Notices, 2014, 1-18.

Jacob, J. M., Rajan, R., Aji, M., Kurup, G. G., Pugazhendhi, A. (2019). Bio-inspired ZnS quantum dots as efficient photocatalysts for the degradation of methylene blue in aqueous phase. Ceramics International, 45(4), 4857-4862.

Jain, P. K., Lee, K. S., El-Sayed, I. H., El-Sayed, M. A. (2006). Calculated absorption and scattering properties of gold nanoparticles of different size, shape, and composition: Applications in biological imaging and biomedicine. Journal of Physical Chemistry B, 110, 7238-7248. doi: 10.1021/jp057170o.

Jans, H., Liu, X., Austin, L., Maes, G., Huo, Q. (2009). Dynamic light scattering as a powerful tool for gold nanoparticle bioconjugation and biomolecular binding studies. Analytical Chemistry, 81, 9425-9432.

Jasim, S. A., Saleh, N. A. (2019). The cytotoxic effect of zinc oxide on colon cancer cell lines in vitro. Indian Journal of Public Health Research and Development, 10, 2638.

Kalpana, V. N., Sirish Kataru, B. A., Sravani, N., Vigneshwari, T., Panneerselvam, A., Devi Rajeswari, V. (2018). Biosynthesis of zinc oxide nanoparticles using culture filtrates of *Aspergillus niger*: Antimicrobial textiles and dye degradation studies. OpenNano, 3, 48-55.

Kern W.V and Rieg S.(2019). Burden of bacterial bloodstream infection—a brief update on epidemiology and significance of multidrug-resistant pathogens.Clinical Microbiology and Infection},{26},151-157,https://doi.org/10.1016/j.cmi.2019.10.031

Khalil, M. N., Abd El-Ghany, M. N., Rodríguez-Couto, S. (2019). Antifungal and anti-mycotoxin efficacy of biogenic silver nanoparticles produced by *Fusarium chlamydosporum* and *Penicillium chrysogenum* at non-cytotoxic doses. Chemosphere, 218, 477-486.

Kołodziejczak radzimska, A., Jesionowski, T. (2014). Zinc oxide—from synthesis to application: A review. Materials, 2833–2881.

Kuruppu, K. A. S. S., Perera, K. M. K. G., Chamara, A. M. R., Thiripuranathar, G. (2020). Flower Shaped ZnO-NPs; Phytofabrication, Photocatalytic, Fluorescence Quenching, and Photoluminescence Activities. Nano Express, 1(2), 020020. doi: 10.1088/2632-959x/aba862.

Lallo da Silva, B., Caetano, B. L., Chiari-Andreo, B. G., Pietro, R., Chiavacci, L. A. (2019). Increased antibacterial activity of ZnO nanoparticles: Influence of size and surface modification. Colloids and Surfaces B: Biointerfaces, 177, 440-447. doi: 10.1016/j.colsurfb.2019.02.013.

Ljaz, F., Shahid, S., Khan, S. A., Ahmad, W., Zaman, S. (2017). Green synthesis of copper oxide nanoparticles using Abutilon indicum leaf extract: Antimicrobial, antioxidant, and photocatalytic dye degradation activities. Tropical Journal of Pharmaceutical Research, 16, 743-753. https://doi.org/10.4314/tjpr.v16i4.2

Nabil, A., Elshemy, M. M., Asem, M., Abdel-Motaal, M., Gomaa, H. F., Zahran, F., Uto, K., & Ebara, M. (2020). Zinc Oxide Nanoparticle Synergizes Sorafenib Anticancer Efficacy with Minimizing Its Cytotoxicity. Oxidative medicine and cellular longevity, 2020, 1362104. https://doi.org/10.1155/2020/1362104.

Majeed, S., Danish, M., Ismail, M. H. B., Ansari, M. T., Ibrahim, M. N. M. (2019). Anticancer and apoptotic activity of biologically synthesized zinc oxide nanoparticles against human colon cancer HCT-116 cell line: In vitro study. Sustainable Chemistry and Pharmacy, 14, 100179. doi: 10.1016/j.scp.2019.100179

Markou, P., & Apidianakis, Y. (2014). Pathogenesis of intestinal *Pseudomonas aeruginosa* infection in patients with cancer. Frontiers in Cellular and Infection Microbiology, 3, 115. https://doi.org/10.3389/fcimb.2013.00115

Meier, B. (2013). Pressure grows to create drugs for superbugs. The New York Times, p.A1.

Mendes, C. R., Dilarri, G., Forsan, C. F., Sapata, V. M. R., Lopes, P. R. M., de Moraes, P. B., Montagnolli, R. N., Ferreira, H., Bidoia, E. D. (2022). Antibacterial action and target mechanisms of zinc oxide nanoparticles against bacterial pathogens. Scientific Reports, 12(1), 2658. doi: 10.1038/s41598-022-06657-y.

Mishra, A., Kumari, M., Pandey, S. (2014). Biocatalytic and antimicrobial activities of gold nanoparticles synthesized by *Trichoderma* sp. Bioresource Technology, 166, 235-242.

Mishra, Y. K., Modi, G., Cretu, V. (2015). Direct growth of freestanding ZnO tetrapod networks for multifunctional applications in photocatalysis, UV photodetection, and gas sensing. ACS Applied Materials & Interfaces, 7, 14303-14316.

Mohd Yusof, H., Mohamad, R., Zaidan, U. H., Abdul Rahman, N. A. (2019). Microbial synthesis of zinc oxide nanoparticles and their potential application as an antimicrobial agent and a feed supplement in animal industry: A review. Journal of Animal Science and Biotechnology, 10, 57. https://doi.org/10.1186/s40104-019-0368-z

Mousa, A. B., Moawad, R., Abdallah, Y., *et al*. (2023). Zinc Oxide Nanoparticles Promise Anticancer and Antibacterial Activity in Ovarian Cancer. Pharmaceutical Research.

Moyer, E., Hardon, A. (2014). A disease unlike any other? Why HIV remains exceptional in the age of treatment. Medical Anthropology, 33, 263-269.

Mozaffari, H. R., Izadi, B., Sadeghi, M., Rezaei, F., Sharifi, R., Jalilian, F. (2016). Prevalence of oral and pharyngeal cancers in Kermanshah province, Iran: A ten-year period. International Journal of Cancer Research, 12, 169-175.

Mozaffari, H. R., Zavattaro, E., Saeedi, M., Lopez-Jornet, P., Sadeghi, M., Safaei, M., Imani, M. M., Nourbakhsh, R., Moradpoor, H., Golshah, A., Sharifi, R. (2019). Serum and salivary interleukin-4 levels in patients with oral lichen planus: A systematic review and meta-analysis. Oral Surgery, Oral Medicine, Oral Pathology, Oral Radiology, 2019.

Mukherjee, P., Roy, M., Mandal, B. P., Dey, G. K., Mukherjee, P. K., Ghatak, J., Tyagi, A. K., Kale, S. P. (2008). Green synthesis of highly stabilized nanocrystalline silver particles by a non-pathogenic and agriculturally important fungus *T. asperellum*. Nanotechnology, 19, 103-110.

Narayanan, K. B., & Sakthivel, N. (2010). Biological synthesis of metal nanoparticles by microbes. Advances in Colloid and Interface Science, 156, 1-13.

Oliveira, A. L., de Souza, M., Carvalho Dias, V. M., Ruiz, M. A., Silla, L., Tanaka, P. Y. (2007). Epidemiology of bacteremia and factors associated with multi-drug-resistant gram-negative bacteremia in hematopoietic stem cell transplant recipients. Bone Marrow Transplantation, 39, 775-781. https://doi.org/10.1038/sj.bmt.1705677

Ong, C. B., Ng, L. Y., Mohammad, A.W. (2018). A review of ZnO nanoparticles as solar photocatalysts: Synthesis, mechanisms, and applications. Renewable and Sustainable Energy Reviews, 81, 536-551. https://doi.org/10.1016/j.rser.2017.08.020

Osmery Vitta, M., Figueroa, M., Calderon, M., Ciangherotti, C. (2020). Synthesis of iron nanoparticles from aqueous extract of *Eucalyptus robusta* Sm and evaluation of antioxidant and antimicrobial activity. Materials Science for Energy Technologies, 3, 97-103.

Padmavathy, N., Vijayaraghavan, R. (2008). Enhanced bioactivity of ZnO nanoparticles: An antimicrobial study. Science and Technology of Advanced Materials, 9(3), 035004.

Pandey, S., Mishra, S. B., & Sharma, M. (2019). Green synthesis and characterization of zinc oxide nanoparticles using Ocimum tenuiflorum (tulsi) leaf extract. Journal of Materials Science: Materials in Electronics, 30(15), 14662-14670.

Parashar, V., Parashar, R., & Sharma, B. A. C. (2009). Parthenium leaf extract mediated synthesis of silver nanoparticles: A novel approach towards weed utilization. Digest Journal of Nanomaterials and Biostructures, 4(1), 45-50.

Parihar, V., Raja, M., & Paulose, R. (2018). A brief review of structural, electrical and electrochemical properties of zinc oxide nanoparticles. Reviews on Advanced Materials Science, 53(2), 119-130.

Patel, H. G., Tabassum, S., & Shaikh, S. (2017). E. coli Sepsis: Red Flag for Colon Carcinoma-A Case Report and Review of the Literature. Case Reports in Gastrointestinal Medicine, 2017, 2570524. https://doi.org/10.1155/2017/2570524

Rajan, A., Cherian, E., & Gurunathan, B. (2016). Biosynthesis of zinc oxide nanoparticles using *Aspergillus fumigatus* JCF and its antibacterial activity. 1, 52-57.

Rana, K. L., Kour, D., Yadav, N., & Yadav, A. N. (2020). Endophytic Microbes in Nanotechnology: Current Development, and Potential Biotechnology Applications. In A. Kumar & V. K. Singh (Eds.), Woodhead Publishing Series in Food Science, Technology

and Nutrition (pp. 231-262). Woodhead Publishing. https://doi.org/10.1016/B978-0-12-818734-0.00010-3

Rasmussen, J. W., Martinez, E., Louka, P., & Wingett, D. G. (2010). Zinc oxide nanoparticles for selective destruction of tumor cells and potential for drug delivery applications. Expert Opinion on Drug Delivery, 7(9), 1063-1077.

Safdar, A., & Armstrong, D. (2001). Infectious morbidity in critically ill patients with cancer. Critical Care Clinics, 17, 531-570, vii-viii. https://doi.org/10.1016/S0749-0704(05)70198-6

Salgado, P., Mártire, D. O., Vidal, G. (2019). Eucalyptus extracts-mediated synthesis of metallic and metal oxide nanoparticles: Current status and perspectives. Materials Research Express, 6, 082006.

Saratale, R. G., Karuppusamy, I., Saratale, G. D., Pugazhendhi, A., Kumar, G., Park, Y., Ghodake, G. S., Bharagava, R. N., Banu, J. R., & Shin, H. S. (2018). A comprehensive review on green nanomaterials using biological systems: Recent perception and their future applications. Colloids and Surfaces B: Biointerfaces, 170, 20-35.

Shabaani, M., Rahaiee, S., Zare, M., & Jafari, S. M. (2020). Green synthesis of ZnO nanoparticles using loquat seed extract; Biological functions and photocatalytic degradation properties. LWT, 134, 110133.

Shah, M., Fawcett, D., Sharma, S., Tripathy, S. K., & Poinern, G. E. J. (2015). Green synthesis of metallic nanoparticles via biological entities. Materials, 8, 7278-7308. https://doi.org/10.3390/ma8115377

Shankar, S. S., Ahmad, A., Pasricha, R., & Sastry, M. (2003). Bioreduction of chloroaurate ions by geranium leaves and its endophytic fungus yields gold nanoparticles of different shapes. Journal of Materials Chemistry, 13, 1822-1826.

Sharifi, R., Khazaei, S., Mozaffari, H. R., Amiri, S. M., Iranmanesh, P., & Mousavi, S. A. (2017). Effect of massage on the success of anesthesia and infiltration injection pain in maxillary central incisors: Double-blind, crossover trial. Dent Hypotheses, 8(3), 61-64.

Sharma, H., Kumar, K., Choudhary, C., Mishra, P., & Vaidya, B. (2016). Development and characterization of metal oxide nanoparticles for the delivery of anticancer drug. Artificial Cells, Nanomedicine, and Biotechnology, 44(2), 672-679.

Sharma, S. C. (2016). ZnO nano-flowers from Carica papaya milk: Degradation of Alizarin Red-S dye and antibacterial activity against *Pseudomonas aeruginosa* and *Staphylococcus aureus*. Optik, 127, 6498-6512. https://doi.org/10.1016/j.ijleo.2016.04.036

Shen, C., James, S. A., de Jonge, M. D., Turney, T. W., Wright, P. F., & Feltis, B. N. (2013). Relating cytotoxicity, zinc ions, and reactive oxygen in ZnO nanoparticle-exposed human immune cells. Toxicological Sciences, 136(1), 120-130.

Sisubalan, N., Ramkumar, V. S., Pugazhendhi, A., Karthikeyan, C., Indira, K., Gopinath, K., Hameed, A. S. H., & Basha, M. H. G. (2018). ROS-mediated cytotoxic activity of ZnO and CeO2 nanoparticles synthesized using the Rubia cordifolia L. leaf extract on MG-63 human osteosarcoma cell lines. Environmental Science and Pollution Research, 25, 10482-10492.

Smith, A. , Oertle, J. and Prato, D. (2014) Cancer and Infectious Causes. Open Journal of Medical Microbiology, 4, 161-177. doi: 10.4236/ojmm.2014.43019.

Stankic, S., Suman, S., & Haque, F. (2016). Pure and multi metal oxide nanoparticles: Synthesis, antibacterial and cytotoxic properties. Journal of Nanobiotechnology, 14, 73.

Subramaniam, V. D., Ramachandran, M., Marotta, F., Banerjee, A., Sun, X. F., & Pathak, S. (2019). Comparative study on anti-proliferative potentials of zinc oxide and aluminium

oxide nanoparticles in colon cancer cells. Acta Biomedica, 90(2), 241-247. https://doi.org/10.23750/abm.v90i2.6939

Sunkar, S., & Nachiyar, C. V. (2012). Microbial synthesis and characterization of silver nanoparticles using the endophytic bacterium Bacillus cereus: A novel source in the benign synthesis. Global Journal of Medical Research, 12, 43-50.

Sunkar, S., & Nachiyar, V. (2013). Endophytes as potential nanofactories. Journal of Biological and Chemical Sciences, 1, 488-491.

Suryanarayanan, T. S., Venkatesan, G., & Murali, T. S. (2003). Endophytic fungal communities in leaves of tropical forest trees: Diversity and distribution patterns. Current Science, 85(4), 489-492.

Tjalsma, H., Boleij, A., Marchesi, J. R., & Dutilh, B. E. (2012). A bacterial driver-passenger model for colorectal cancer: Beyond the usual suspects. Nature Reviews Microbiology, 10, 575-582. https://doi.org/10.1038/nrmicro2819

Verma, V. C., Anand, S., Ulrichs, C., & Singh, S. K. (2013). Biogenic gold nanotriangles from *Saccharomonospora* sp., an endophytic actinomycetes of Azadirachta indica A. Juss. International Nano Letters, 3, 21.

Viscoli, C., Varnier, O., & Machetti, M. (2005). Infections in patients with febrile neutropenia: epidemiology, microbiology, and risk stratification. Clinical Infectious Diseases, 40(Suppl 4), S240-S245. https://doi.org/10.1086/427329

Vivek, R., Muthuchelian, K., Gunasekaran, P., Kaveri, K., & Kannan, S. (2012). Green biosynthesis of silver nanoparticles from Annona sequamosa leaf extract and its *in vitro* cytotoxic effect on MCF-7 cells. Process Biochemistry, 47, 2405-2410.

Wijesinghe, U., Thiripuranathar, G., Iqbal, H., & Menaa, F. (2021). Biomimetic synthesis, characterization and evaluation of fluorescence resonance energy transfer, photoluminescence and photocatalytic activity of zinc oxide nanoparticles. Sustainability, 13(4), 2004.

Wong, C. Y., Al-Salami, H., & Dass, C. R. (2017). Potential of insulin nanoparticle formulations for oral delivery and diabetes treatment. Journal of Controlled Release, 264, 247-275.

Ying, S., Guan, Z., Ofoegbu, P. C., Clubb, P., Rico, C., He, F., & Hong, J. (2022). Green synthesis of nanoparticles: Current developments and limitations. Environmental Technology & Innovation, 26, 102336. ISSN 2352-1864

Yoo, A., Lin, M., & Mustapha, A. (2021). Zinc oxide and silver nanoparticle effects on intestinal bacteria. Materials, 14, 2489.

Yousefi, M., Gholami-Shabani, M., & Salavati-Niasari, M. (2018). The green synthesis of ZnO nanoparticles using endophytic fungi, Fusarium solani. Journal of Inorganic and Organometallic Polymers and Materials, 28(6), 2329-2335. https://doi.org/10.1007/s10904-018-0916-x

Zak, A. K., Razali, R., Majid, W. H., & Darroudi, M. (2011). Synthesis and characterization of a narrow size distribution of zinc oxide nanoparticles. International Journal of Nanomedicine, 6, 1399-1403.

Zhang, L., Jiang, Y., Ding, Y., Povey, M., & York, D. (2007). Investigation into the antibacterial behaviour of suspensions of ZnO nanoparticles (ZnO nanofluids). Journal of Nanoparticle Research, 9, 479-489.

Zhou, J., Xu, N. S., & Wang, Z. L. (2006). Dissolving behavior and stability of ZnO wires in biofluids: A study on biodegradability and biocompatibility of ZnO nanostructures. Advanced Materials, 18(18), 2432.

Zubair, N., & Akhtar, K. (2020). Morphology controlled synthesis of ZnO nanoparticles for in-vitro evaluation of antibacterial activity. Transactions of Nonferrous Metals Society of China, 30(6), 1605-1614.

تقييم مقارن للأنشطة المضادة للسرطان والبكتيريا لجسيمات ZNO المصنعة بواسطة الفطريات الداخلية وجسيمات ZNO النانوية المصنعة كيميائيا

* سامح عزت حماد [1]، حسين حسني الشيخ [1]، محمود نور الدين الروبى[2]، مروة عبد العزيز مصطفى [3].

[1]قسم النبات والأحياء الدقيقة، كلية العلوم (بنين)، جامعة الأزهر، 11884 نصر، القاهرة، مصر.

[2] قسم بيولوجيا السرطان، المعهد القومي المصري للأورام، جامعة القاهرة، قصر العيني، القاهرة، مصر.

[3]علم الأحياء الدقيقة الطبية، المركز الإقليمي لعلم الفطريات والتكنولوجيا الحيوية، جامعة الأزهر، القاهرة، مصر.

* البريد الالكتروني الرئيسي للباحث : drsameh206@yahoo.com

اعتمادا على منظمة الصحة العالمية، لا تزال مقاومة المضادات الحيوية والعلاجات المحدودة المضادة للسرطان ومضادات الميكروبات تشكل تحديات صحية خطيرة في جميع أنحاء العالم. تعاني فعالية الأدوية الحالية من مشاكل مثل عدم كفاية الذوبان والاستقرار والآثار الجانبية. لإنشاء علاجات فعالة ويمكن الاعتماد عليها ضد مقاومة المضادات الحيوية والأمراض القوية، هناك حاجة إلى تقنيات واستراتيجيات جديدة. أظهرت العديد من الجسيمات النانوية المعدنية التي تم تصنيعها عن طريق التخليق الأخضر أو التخليق الكيميائي، مثل الذهب (Au) وأكسيد الزينك (ZnO) وغيرها، آثارا بيولوجية واعدة ضد الأورام الخبيثة وطائفة واسعة من الأمراض الميكروبية التي تسببها البكتيريا المقاومة للأدوية المتعددة.

تبحث هذه الرساله عن إيجاد طرق جديدة لانتاج الجزيئات النانوية بطريقة صديقه للبيئة واستخدامها للقضاء على الامراض السرطانية وكذلك كمضاد للبكتريا الممرضة (المقاومة للمضادات الحيوية)

تم استخدام تقنية التخليق الحيوي (الكيمياء الخضراء) الصديقة للبيئة لإنتاج جسيمات أكسيد الزنك النانوية (ZnO NPs) عن طريق استخدام الفطريات الداخلية المتعايشه مع النباتات المضيفة. تم عزل 13 عزله من الفطريات الداخلية لاوراق نبات *Eucalyptus sideroxylon* وتم تعريف عزله واحده عن طريق التعريف الظاهري والجيني والتي كان لها القدرة على انتاج جزيئات أكسيد الزنك النانوية وهي *Fusarium chlamydosporum* MW341592.1 وتم عمل توصيف لهذه الجزيئات بالتحليل الطيفي للأشعة المرئية وفوق البنفسجية، وحيود الأشعة السينية (XRD)، وتشتت الضوء الديناميكي (DLS) ، والمجهر الإلكتروني الانتقالي (TEM) ، والتحليل الطيفي للأشعة السينية المشتتة للطاقة (EDX). أظهرت أطياف امتصاص الأشعة المرئية وفوق البنفسجية ل ZnO NPs المنتجة نطاقات في منطقة الأشعة فوق البنفسجية عند (305) نانومتر. كما كشف المجهر الإلكتروني النافذ TEM عن جزيئات كروية الشكل ومتوسط أحجام 19.3 نانومتر.

علاوة على ذلك تم عمل مقارنة بين جزيئات أكسيد الزنك النانوية المصنعة حيويا والمصنعة كيميائيا، حيث أظهرت جزيئات الزنك النانويه المصنعه حيويا نشاطا اكبر مضاد للبكتيريا المقاومه للمضادات الحيوية *Escherichia coli* و *Pseudomonas aeruginosa*

حيث بلغ تركيز الحد الأدنى للتثبيط (MIC) لجزيئات أكسيد الزنك الصناعية كيميائياً ضد بكتيريا (*P. aeruginosa*) قيمة (7.81 ميكروغرام/مل)، بينما تركيز الحد الأدنى للتثبيط (MIC) ضد بكتيريا (E. coli) قيمة (3.9 ميكروغرام/مل)

وبلغ تركيز الحد الأدنى المثبط (MIC) لجزيئات أكسيد الزنك النانوية المصنعة حيويا ضد بكتيريا *P. aeruginosa* كان (1.95 ميكروغرام/مل)، بينما أظهرت أن تركيز الحد الأدنى المثبط (MIC) ضد بكتيريا *E.coli* كان (0.98 ميكروغرام/مل)."

كما أظهرت الدراسه أن نشاط الجسيمات النانوية يقلل من عدد خلايا سرطان القولون البشري HCT-116 وخلايا سرطان الأمعاء البشرية CACO2،

حيث أظهرت النتائج تأثير مضاد لخلايا سرطان الأمعاء CACO2 تركيزات التثبيط (IC50) تبلغ 3.7 ميكروغرام/مل بالنسبة لجزيئات أكسيد الزنك النانوية المصنعة حيويا بينما كانت 6.07 ميكروغرام/مل بالنسبة لجزيئات المصنعة كيميائيا.

كما وجدت الدراسة تأثيراً مضاداً لخلايا سرطان القولـون البشـري HCT-116 حيـث بلغـت تركيـزات التثبـيط (IC50) تبلغ 5.6 ميكروغرام/مل بالنسبة لجزيئات أكسيد الزنك النانوية المصنعة حيويا بينما كانت 7.51 ميكروغرام/مل بالنسبة لجزيئات المصنعة كيميائيا.

وكانت الجزيئات النانويه المصنعة حيويا اكثر نشاطا كمضاد للسرطان عن المصنعة كيميائيا.

الكلمات المفتاحية: جسيمات أكسيد الزنك النانوية ، التخليق الحيـوي ، الفطريـات الداخليـة ، النشـاط المضـاد للبكتيريـا ، النشاط المضاد للسرطان